EPFL

IPESE
Industrial Process
and Energy Systems
Engineering

Energy Sciences and Technology

District energy network potentials in a city territory

Master Project

Author:
Raphaël BRIGUET

Supervisors:
Prof. François MARÉCHAL
Prof. Jessen PAGE
Jonas SCHNIDRIG

External Expert:
Etienne MOULIN

Industrial Processes and Energy Systems Engineering
Ecole Polytechnique Fédérale de Lausanne

Sion, 2nd September 2022

Contents

Abstract

Keywords: Urban system, Geographical database, District heating network, Fifth-generation district heating and cooling, Industry integration, Sustainable energy supply

Following the Covid crisis and the war in Ukraine, the rise of fossil fuels prices demonstrates the insecurity of the supply in addition to the adverse impact it has on the environment. These crises could lead to a global shift in the strategy of building heating. Renewable systems are promising alternatives to fossil fuel heating system. One of them is the District Heating Network that has the advantages of recovering the waste heat from the industry. In the context of a neutral carbon objective set by the aluminium factory *Novelis*, the city of Sierre is interested in investigating the possibility of developing a District Heating Network (DHN). This study develops a method to design a network between a heat source and a city, based only on open data building's inventory. The method, applied to the case study of Sierre, shows that, coupled with heat pumps, the DHN could reduce the heating emissions of the connected buildings, between 88% and 96 % and that 50% of the *Novelis*' heat is recoverd when half of the city is connected to the network. In addition to that, using new generation of DHN, like CO_2 based network makes possible to supply cold with the same infrastructure.

Acknowledgments

This master's thesis is the final step of my journey at EPFL. I am honored to have been able to conclude this chapter within the IPESE laboratory. I would like to thank first of all François Maréchal, who welcomed me with great kindness and allowed me to work on exciting subjects. I am also grateful to him for having offered me the opportunity to participate in the ECOS conference as part of my semester project.

I would like to thank Jessen Page and Etienne Moulin for having followed me throughout this work.

Thanks to Cédric Dorsaz and Pierre-Jean Duc for their interest in the work and for their availability.

Thank you Jonas for your generous help, your kindness and your support throughout this unforgettable year spent at IPESE.

Of course I thank the people from lab with whom I really appreciated collaborating: Xiang, Dorsan, Cédric, Michel, Luc, Joseph.

I conclude by thanking Teodora for her patience and her devotion so precious to the writing of this report.

Raphaël Briguet

List of Figures

List of Tables

Chapter 1

Introduction

1.1 Background

In Switzerland, 60% of the heating demand is supplied by fossil fuels [5]. Following the Covid crisis and the war in Ukraine, the rise of fossil fuels prices demonstrates the insecurity of the supply in addition to the adverse impact it has on the environment. These crises could lead to a global shift in the strategy of building heating. Renewable systems like heat pumps are promising alternatives to fossil fuel heating system. However, some aspects are slowing down the transition towards greener heat production supply. First, these modern technologies often require large investment cost that discourages the owner. This amount also depends on the level of modification and renovation that the building requires. Another limiting factor is the difficulty to find common ground among co-owners or between tenants and owners. Switzerland has one of the lowest rate of owners in Europe. In 2020, only 36.2% of Swiss households are owners, a number that also includes 11.8% of co-ownership [6]. The centralization of the heat production is an efficient way to shift to renewable energy without the necessity of a significant investment from the consumer.

The world leader in aluminium rolling and recycling, *Novelis*, plans to be a carbon-neutral company by 2050 or sooner [7]. For this purpose, *Novelis* announced in February 2022 that the factory based in Sierre (Valais-CH) will be the development site of this recent objective, which is to reach carbon neutrality of the plant by 2030 [8]. This site is *Novelis*' most advanced factory in terms of aluminium sheet produced for the automobile manufacturing and includes already a Research & Innovation Center that focuses on the development of sustainable and innovating manufacturing technologies. In addition, the availability of renewable energy makes the site of Sierre an ideal candidate for innovation. In this perspective, *Net Zero Lab Valais* has been launched and will be the structure in charge of developing solutions to reach the aforementioned objective. This project consists in a collaboration of different actors in the energy field namely *Novelis*, the local energy supplier *Oiken*, *HES-SO Valais-Wallis* and *EPFL*.
In this context, the city of Sierre, which is greatly engaged in the sustainability of the city and certified *Cité de l'énergie Gold* by the *European Energy Award* [9], is interested in investigating the possibility

of developing a DHN. The principle consists of supplying heat to households through underground pipes, powered by a centralized production or/and by the recovery of industrial waste heat. On the other side, in order to reach the carbon-neutral objective, *Novelis* has to recycle as much as possible the produced heat. The integration of *Novelis* to the energy system of the city is therefore a convenient concept for both sides.

In this respect, this study has the objective of analysing the different pathways to reduce on the one hand Sierre's carbon footprint linked to the heating demand and on the other hand, to valorize the heat released by *Novelis* for achieving carbon neutrality. Throughout this work, a methodology to design a DHN is developed and applied to the case study of Sierre.

1.2 State of the art

1.2.1 Heating and cooling demand in Urban area

Dong et al. [10] shows that the energy demand of a building can be predicted with a confidence interval of 90% by using only the outdoor temperature. Then, Girardin [2] uses the energy signature of buildings of different affectations and ages to define the heating and cooling needs of typical buildings. The latter are then scaled to define the demand of any building. Suciu [11] highlights the difficulty to gather data in residential sectors. A hybrid method is consequently used to model the energy demand of buildings.

1.2.2 District heating and cooling

[12] shows the potential of using low temperature district heat network compared to conventional DHN. Smart thermal grids are defined as the way to share the heat between buildings (neighbourhood of city) with high synergy, integrating renewable energy technologies and storage systems. Some relevant challenges are highlighted like the ability to supply low-temperature district heating to existing buildings, reduce the grid losses, valorize low T waste heat and integrate sustainable energy technologies. However, this low temperature network cannot supply cold. Weber and Favrat [13] introduces the concept of using CO_2 as fluid for district heating network. The fluid is compressed at an average pressure of 50 bar and around a saturation temperature between 12 and 18 °C. Henchoz [3] and Henchoz et al. [14] demonstrate a potential of reducing the energy consumption by 84% for a district in Geneva compared to a full decentralized scenario. Suciu [11] and Suciu et al. [15] focus on the integration of low temperature industry waste and natural heat source to a CO_2 network with the objective to attain a carbon neutral and autonomous energy system.

Girardin [2] evaluates the cost of using centralized energy production by integrating efficient conversion technologies. A function for estimating pipe length is presented. Unternährer et al. [16] presents a methodology to determine the integration of DH network in urban energy system. The districts are determined using Integer Linear Programming (ILP) that aims to minimize the piping length. Graph

theory and routing methods are then used to give a realistic estimation of the network length by following roads. Once the districts are defined, a MILP optimization is employed in order to obtain the cost-effectiveness of integrating centralized energy conversion technologies.

1.3 Problem Statement

In parallel to the process optimization of *Novelis*' factory based in Sierre, the potential of integrating the factory to the city can be evaluated. The neutral carbon objective intended by *Novelis* depends on the capacity of the city to absorb the heat waste. Therefore, the objective is to estimate the possibilities for *Novelis* and Sierre to be complementary.

1.3.1 Research questions

With the aim to answer the question of *Novelis*' integration to Sierre, the following questions can be asked:

- How can the city's energy demand be estimated?
- What are the different solutions to distribute heat at a city scale ? What are their strengths and weaknesses ?
- How to select the buildings that should be connected to the network ?
- What is the cost of the DHN's infrastructure ?
- How can an industry be integrated in the system ?
- Are auxiliary units necessary ? What are their sizes ?
- Which type of DHN is the most adapted ?

1.3.2 Objectives

In order to respond to the research questions, the study uses the following strategy:

1. Use a statistical approach to estimate the energy demand of a building based on reference buildings. The results are validated through comparison with other studies.
2. Present the differences between the generations of District Heating Network and select some of them to be compared.
3. Define the methodology to determine the size of the pipes, the losses and the price in function of the required power and the level of temperature. A formula calibrated on the city gives an estimation of the network length within a district
4. The study uses graph algorithm to connect the districts together with the industry and proceeds to a routing optimization for obtaining a realistic estimation of the piping length.

5. The hourly heat demand profile of the buildings are used to dimension the auxiliary unit and compute its load profile

6. The key performance indicators allows us to compare the different configurations of network, like energy efficiency, cost and Global Warming Potential.

The objective (1) is discussed in Section 2.1. Section 2.2 focuses on objective (2) and (3). Then, the subject (4) and (5) are presented in Section 2.3, and finally, the Results part (Section 3) presents the objective (6).

1.3.3 Approach

The methodology developed in this study is exclusively based on open Swiss buildings inventory provided by the Swiss Confederation. No specific data or measurement of the case study is required. This allows us to apply the methodology to any city or industry. Despite the lower accuracy compared to a more in-depth survey, this way to proceed provides a quick overview of the potential and price of integrating industry to any city, based on the energy profile's needs.

1.4 Project Background

This project has been realized as Master Thesis within the Energy Science and Technology Master program at Ecole Polytechnique Fédérale de Lausanne (EPFL) in the laboratory Industrial Processes and Energy Systems Engineering (IPESE) directed by Prof. François Maréchal. The thesis is supervised by Prof. Jessen Page.

Chapter 2

Methodology

2.1 Evaluation of the energy demand

The evaluation of a building's energy needs is essential when studying the possibility of integrating an energy system at a building's or district scale. The validity of these data is required since results are highly dependent on it. Different strategies can be used to determine the energy demand (bottom up or top down approach). By the end of 2016, on Sierre's mandate, *Amstein+Walthert SA* made the Territorial Energy Master Plan. This report gives a detailed analysis of the city concerning the production and distribution of energy and the potential resources of the territory. It has as an objective to help the city for the decision-making related to the city's energy system.

This section aims to evaluate the demand of the city, using the tool developed by IPESE. It allows us one the one side to generate an updated version of the energy evaluation and on the other side, to assess the validity of the tool by comparing it to the study conducted by *Amstein+Walthert* and by underlining the divergent assumptions.

2.1.1 Qbuildings

Qbuildings is a Python tool developed in the context of the PhD thesis of Girardin [GIRADIN] and used now by the *IPESE* lab. Based on Geographic Information System, the program aims to evaluate, with a statistical approach, the energy demand of buildings situated in any location where the data are available. This section is presenting the methodology applied by the *Qbuildings*.

Building inventory

The first step of the process is to collect the data used to identify the positions and characteristics of the buildings. They are mainly based on three databases:

- **RegBL** : geographic point containing information like EGID, affectation, date of construction, number of floor, ...As defined by the Federal Statistical Office (FSO) [17], a RegBL point is

linked to one EGID, which is the identification number of one residence address. A large building can, therefore, contain several RegBL points.

- **SwissTLM3D** : 2D polygon representing the footprint of the buildings.
- **SwissBuildings3D** : 3D modelling of the buildings, giving information on the orientation of the roofs and area of the facades.

For characterizing one building, these data are grouped and aggregated by location and the three of them are necessary to completely define a building. As it can be noted in Figure 2.1 and 2.2, several **RegBL** points can be found in a single footprint, meaning that the building has multiple affectations (e.g housing and commercial) or multiple entrance. However, when one of these three elements is missing, the building cannot be modelled. It mostly occurs when footprint and RegBL are not matching, which can be explained by the fact that some of the data can be outdated or misreported.

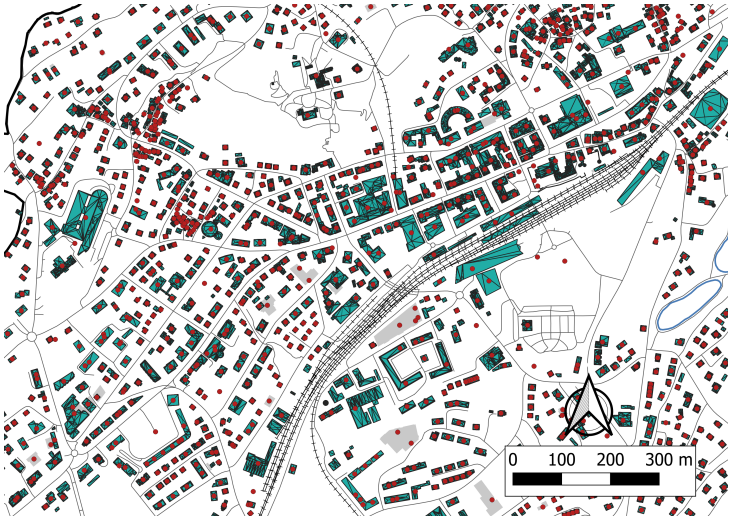

Figure 2.1: City center of Sierre. The blue buildings represent the 3D model from **SwissBuildings3D**. The **RegBL** data are shown by red dots. The grey buildings correspond to the footprint from **SwissTLM3D** and are visible in this map when the 3D model is not available.

Building's energy signature

The evaluation of the energy demand of a building is challenging. The measurements provide accurate data, but are however a very time-consuming and expensive process. In addition, it is not allowed to proceed to the measurement of a building without the agreement of the consumer.
The statistical approach, which is used in this study, has the advantages of being a quick and efficient way to analyse a large amount of buildings. The heat demand Q^{SH+HW} of a building includes the needs for Space Heating (Space Heating (SH)) and Hot Water (Hot Water (HW)) :

$$Q^{SH+HW} = Q^{SH} + Q^{HW} \qquad \text{[kWh]} \tag{2.1}$$

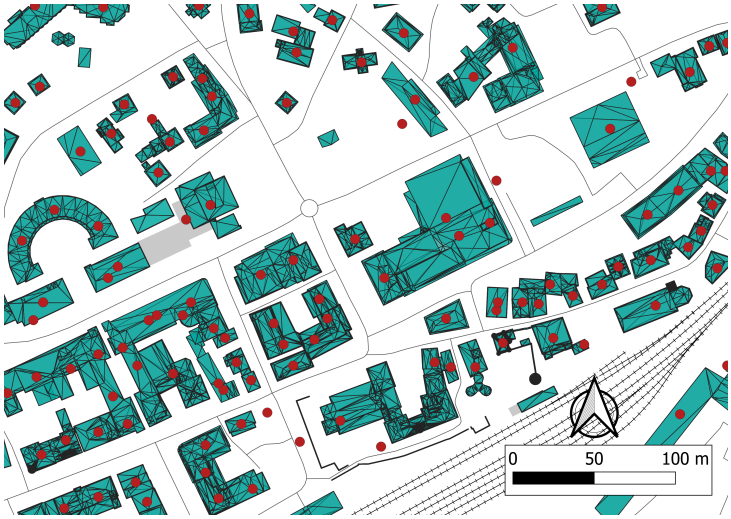

Figure 2.2: Some RegBL points (red points) are located outside the buildings. It can be explained either by the fact that the footprint of the buildings is missing or that the point is misplaced.

Qbuildings provides, among other results, an hourly profile of the SH and HW demand, the required temperature of supply and the size of the utility that needs to be installed. Q, expressed in kWh, refers to the heat, while $\dot{Q}$, in kW, designates a heat transfer rate.

Hot Water The needs for Hot Water (HW) are considered to be constant all along the year and the daily profile of the demand is not taken into account.
The consumption is based on a typical daily consumption of Hot Water per capita provided by the 2024 Standard. The latter also estimates the density of occupant per type of buildings, which allows us to compute the HW needs of a building.

Space Heating *Qbuildings*' strategy to estimate the SH demand consists in creating a set of data that characterizes the demand of typical buildings. For every building whose demand needs to be estimated, the program refers to the corresponding reference building. The heating signature is defined by two coefficients: k_1 and k_2.

In order to define these coefficients, it is first of all necessary to express the heat flow balance of the building. The heat flows are illustrated in Figure 2.3, and the balance is given by Equation (2.2).

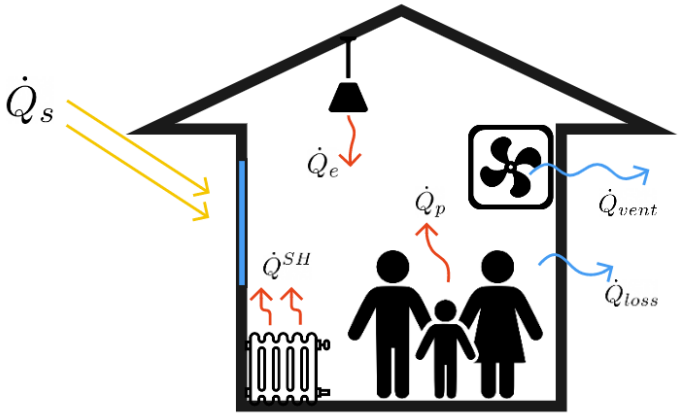

Figure 2.3: The figure describes the heat flows within a building. In addition to the heat exchanged with the outside through the ventilation $\dot{Q}_{vent}$, the walls $\dot{Q}_{loss}$ and solar irradiation $\dot{Q}_s$, the heat released by the electrical facilities $\dot{Q}_e$ and by the building's occupants $\dot{Q}_p$ are also taken into account.

$$\dot{Q}^{SH} + \dot{Q}_s + \dot{Q}_p + \dot{Q}_e - \dot{Q}_{vent} - \dot{Q}_{loss} = 0 \qquad [\text{kW}] \tag{2.2}$$

The heat losses related to the transmission through the wall $\dot{Q}_{loss}$ and to the air renewal $\dot{Q}_{vent}$ can be considered to be proportional to the difference between the inside and outside temperature. The ventilation coefficient K_{vent} and envelope coefficient K_{loss}, expressed in $[\frac{kW}{K}]$ are used to write the following equation:

$$\dot{Q}^{SH} + \dot{Q}_s + \dot{Q}_p + \dot{Q}_e + (K_{vent} + K_{loss}) \cdot (T_0 - T_i) = 0 \qquad [\text{kW}] \tag{2.3}$$

with $\dot{Q}_{vent} = K_{vent} \cdot (T_0 - T_i)$ and $\dot{Q}_{loss} = K_{loss} \cdot (T_0 - T_i)$.

Then, the space heating demand $\dot{Q}^{SH}$ can be isolated. Moreover, all heat flows are assumed to be proportional to the floor area of the building. Hence, Equation (2.3) can be expressed per square meter of floor area as:

$$\dot{q}^{SH} = -(k_{loss} + k_{vent})(T_0 - T_i) - (\dot{q}_s + \dot{q}_p + \dot{q}_e) \qquad [\text{kW/m}^2] \tag{2.4}$$

Assuming a constant intern temperature, the equation is rearranged as a linear expression of the outside temperature T_0. In addition to that, the equation can be written using $k_1 = -(k_{loss} + k_{vent})$ $[\text{kW/m}^2]$:

$$\dot{q}^{SH} = k_1 \cdot T_0 - (k_1 \cdot T_i + \dot{q}_s + \dot{q}_p + \dot{q}_e) \tag{2.5}$$

And finally, k_2, the constant term of the linear equation is $k_2 = -(k_1 \cdot T_i + \dot{q}_s + \dot{q}_p + \dot{q}_e)$:

$$\dot{q}^{SH} = k_1 \cdot T_0 + k_2 \tag{2.6}$$

The total heat demand of a building with a floor area A_f can be calculated with:

$$\dot{Q}^{SH+HW} = \dot{q}^{SH} \cdot A_f + \dot{Q}^{HW} \tag{2.7}$$

$$= (k_1 \cdot T_0 + k_2) \cdot A_f + \dot{Q}^{HW} \tag{2.8}$$

The thermal load $\dot{q}^{SH}$ indicates the power needed in function of the outside temperature. The signature coefficient k_1 and k_2 of a specific building can then be defined using measurements of the heating production at different period of the year. Hence, a linear regression is used to assign a value to the coefficient. Figure 2.4, from [2], illustrates the regression of the measures. The temperature at which the line crosses the x-axis indicates the threshold temperature at which the heating system is turned on. [2] used the measurement of 50 buildings of Geneva to define the signature coefficient k_1 and k_2 for 80 types of buildings, which are available in the cited thesis. Figure 2.5 shows the signature of every typical building, including the cooling signature.

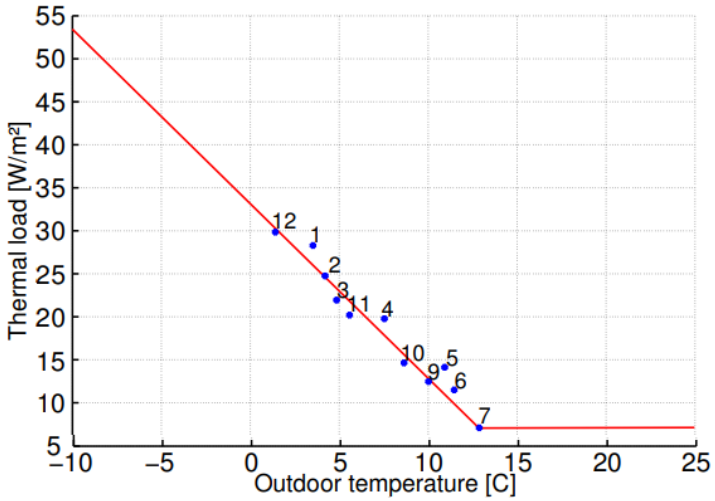

Figure 2.4: The monthly heating measurements of a building in Neuchâtel are represented by blue dots. The regression (red line) allows us to attribute the signature of the building defined by k_1, the slope of the line and k_2 the constant.

2.1.2 Territorial Energy Master Plan of the city of Sierre

As a member of the *Cité de l'Energie*, the city defines its objectives according to an Energy Policy Program. For this purpose, the elaboration of the Territorial Energy Master Plan (TEMP) constitutes the first step of the program. Published in 2016, the latter aims to first analyse the current city's energy situation, then assess the potential of using renewable energy sources in the territory and finally suggest strategies in terms of energy supply and mobility for different scenarios. This section focuses on highlighting the most relevant analyses and results given by the TEMP.

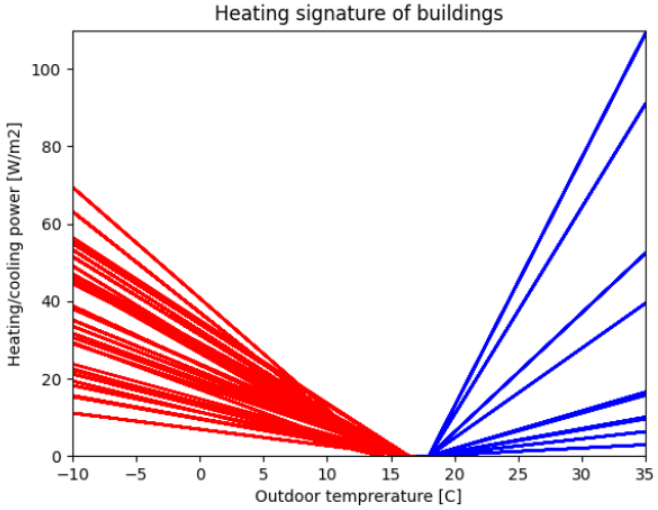

Figure 2.5: The red lines refer to the need of heating while the blue ones the cooling demand.

Building inventory

In addition to the **RegBL**, the Territorial Energy Master Plan (TEMP) also uses real data, provided by the city or by *Oiken*, the local company in charge of the energy distribution. However, for the sake of data security, the consumptions of gas, water and electricity are not available for every a household, but only the consumption of an entire district. In addition to that, the TEMP notes, without further details, that a part of the measurements they have proceeded to were misreported, thus making them unusable. The company also mentions that the consumption of heating oil or wood pellet remains unknown. Nevertheless, the data collected were used to calibrate the model.

Space Heating

The TEMP does not feature many quantitative details regarding the methodology for estimating the heating demand. Only the specific heat consumption of a typical collective housing is presented. These reference data are provided by an internal study concerning the building of the city of Sion. The report mentions that the consumption of other types of buildings is adapted from the collective housing signature using the norm SIA 380/1. The aggregated consumption data collected by *Oiken* are used to calibrate the model. No further details are given concerning the methodology. The heating system is categorized into 3 temperatures of supply: 70 C, 55C and <40C. The category is attributed in function of the period of construction and the renovation.

Hot Water

The HW specific needs ([kWh/m2/y]) as well as the electricity consumption (heating excluded) are also provided by the SIA 380/1 and depend on the affectation of the building.

Table 2.1: Proportion of data used to define buildings

	Last update	Available	Used	Ratio of data used
SwissTLM3D	2016	3323	2420	73 %
RegBL	2022	3498	3180	91 %

Table 2.2: Comparison of the buildings inventory

	Qbuildings	TEMP
Number of buildings	2420	2718
Footprint area [km^2]	2.30	2.08

2.1.3 Results and Comparison

Buildings inventory

As mentioned in Section 2.1.1, *Qbuildings* needs 3 elements in order to characterize a building, meaning that, like illustrated in Figure 2.1, not every building can be defined. Table 2.1 summarizes the proportion of the data used to model the buildings. Only 74% of the building footprints (SwissTLM3D) of Sierre can be completely characterized. The remaining 26% have, in most cases, no **RegBL** points attributed. The **RegBL** points are either not available yet or are mislocated. It can be noted that the large part of these non-used footprints are small buildings, meaning that in terms of ERA, it represents only a small share. Concerning the register data, 91% of the **RegBL** are used while the rest are not matching with the footprint. For its part, **SwissBuilding3D** is less problematic: only 3% of the building footprints cannot be defined as the 3D model is not available. It is important to note that, although the last version of **SwissTLM3D** and **SwissBuilding3D** have been published in 2022, the data of Valais only dates from 2016. Finally, as described in Table 2.2, *Qbuildings* provides results for 2420 buildings while the TEMP reaches 2718 in total. Despite this, *Qbuildings* has a total footprint area 10% higher than what is reported by the TEMP. This difference can be explained by the fact that the buildings missing in *Qbuildings*' results represents only a small share of the total footprint. Moreover, *Qbuildings* uses more recent data and then takes into account new constructions, leading to an expected increase of the footprint.

Affectation of buildings

In both cases, the affectation of buildings mainly relies upon the **RegBL** data. Figure 2.6 confirms that the distribution of the affectation is converging. There is, however, a difference concerning administrative buildings. It can be first explained by the fact that administrative areas are often situated in buildings with multiple affectations (e.g. collective housing/administrative) and only buildings with a unique affectation are presented in the pie chart of *Qbuildings*.

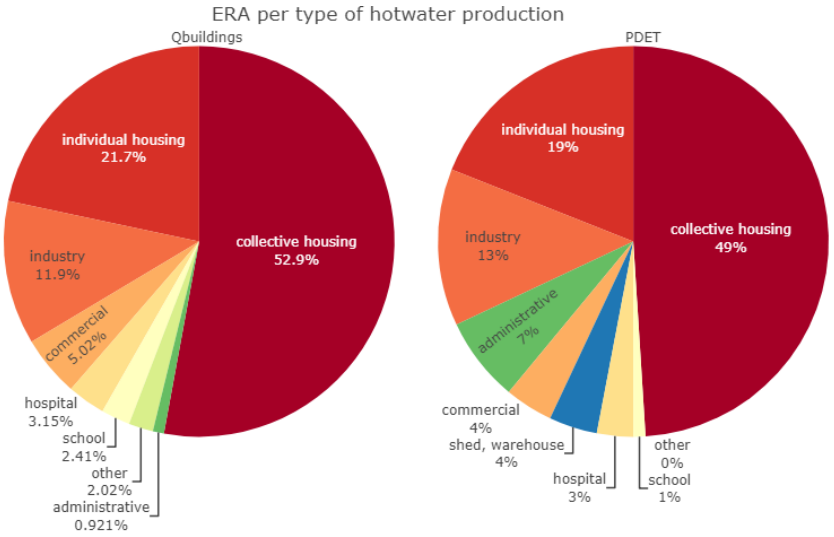

Figure 2.6: Repartition of the ERA by affectation

Energy reference area

The gross floor area A_{gross} is given by the footprint area A_{gnd} multiplied by the number of floor n_{floor}. Then, the Energy Reference Area (ERA), which indicates the heated surface of the building, is deduced from A_{gross}, which is multiplied by a coefficient factor f_{gnd}. The ERA is a key element in the analysis since the energy demands, such as HW and SH are proportional to the ERA, so to the coefficient f_{gnd}.

$$A_{ERA} = A_{gnd} \cdot n_{floor} \cdot f_{gnd} \tag{2.9}$$

$$= A_{gross} \cdot f_{gnd} \tag{2.10}$$

As it is done by *Qbuildings*, the TEMP uses a coefficient f_{gnd} when the real data are not available. As shown in table 2.3, the coefficient used by *Qbuildings* is 16.25 % higher. Since the signature of a building is linearly proportional to the area, this difference directly affects the total demand. However, it must be noted that the value initially used by *Qbuildings* was applied to a city with a high density of buildings, like Geneva, which can indeed justify the high f_{gnd} coefficient. In the case of Sierre, the buildings being significantly smaller than in Geneva, the ERA factor needs to be smaller.

Table 2.3: Gross floor area coefficient

	TEMP	Qbuildings	Deviation
f_{gnd}	0.8	0.93	+16.25 %

Required supply temperature for heating

The requirements in terms of insulation and sophistication of heating technologies are some of the reasons that lead to the reduction of the required temperature for space heating. In fact, older build-

ings used to be equipped with radiators while more recent ones tend to opt for floor heating or active slab. The increase of the exchange area with the room helps to reduce the temperature in the heat exchanger.

Both methodologies attribute the temperature according to the period of construction. However, the profiles are different. Figure 2.7 shows the variation of the design temperature of both methods. In contrast to *Qbuildings* that considers mainly two temperature levels for original buildings, the TEMP has three levels, namely 40, 55 and 70°C. The data have no direct impact on the estimation of the energy demand, but constitutes an important component for decision-making when considering technology integration like district heating. Figure 2.9 and 2.8 show the required temperature for Sierre and how it is distributed. It can be noted that the city center is mostly supplied at high temperature. The low temperature represents only 12-13% of the ERA.

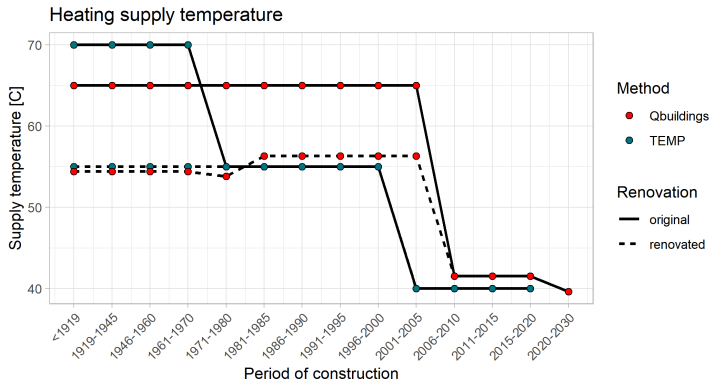

Figure 2.7: The design temperature for a heating system depends on the period of construction. The renovation implies a reduction of the required temperature.

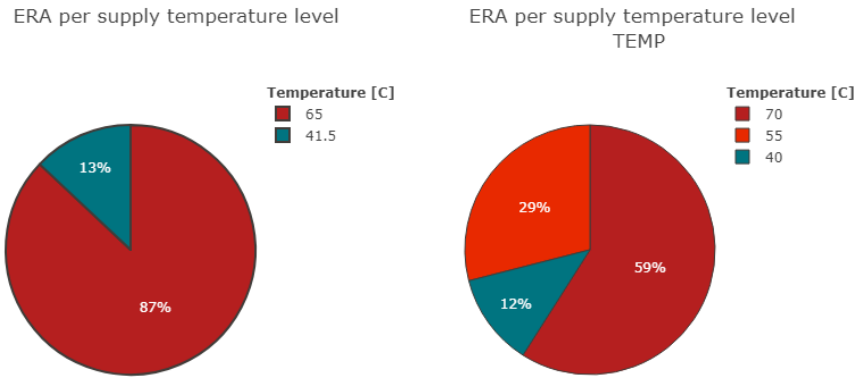

(a) (b)

Figure 2.8: Distribution of the ERA in function of the heating supply temperature for the buildings of Sierre.

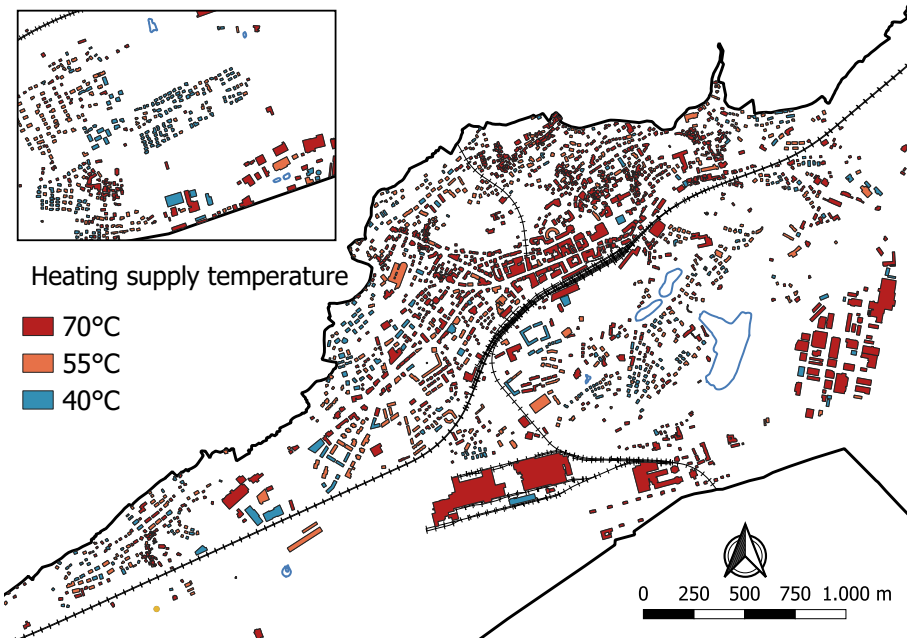

Figure 2.9: Map of Sierre classified by heating supply temperature

Space Heating

The typical heating signature is defined by the affectation and period of construction of buildings. Figure 2.10 features the signatures used by both approaches. As mentioned earlier, *Qbuildings* has defined the typical signature using measurement of Geneva, while the TEMP uses the 380/1 Norm calibrated with real data. Being more optimistic, the *Qbuildings* signature is 19% to 53% lower than the TEMP's one. One element that can explain this significant difference is the following: the reference buildings from Geneva are municipal facilities that are regularly monitored. Their heating system is consequently optimized, leading to smaller specific heat demand. Moreover, the type of architecture can differ from Geneva to Sierre which could make a difference in terms of consumption. For example, a larger building tends to have a lower specific heat demand per square meter since the relative area of exchange with the exterior is smaller. Finally, the average area per capita is smaller for Geneva than Valais. The heat released by the occupant q_p is therefore larger, reducing the heating needs.

The total annual SH demand can be found in Table 2.4. It can be noted that the total demand Q^{SH} difference is low since the specific demand q^{SH} deviation is compensated by the ERA difference.

Table 2.4: Sierre's annual Space Heating needs.

	TEMP	Qbuildings	Difference
ERA [m2]	$1.66 \cdot 10^6$	$2.14 \cdot 10^6$	+ 28 %
Q^{SH} [GWh/y]	196.5	201.2	+ 2 %
q^{SH} [kWh/m^2/y]	118.4	94.0	- 20 %

Table 2.5: Comparison of specific heating needs for a collective housing

Period of construction	TEMP [kWh/m2/an]	Qbuildings [kWh/m2/an]	deviation [%]
<1919	140	102	-27.1
1919-1945	156	114	-26.9
1946-1960	160	114	-28.7
1961-1970	156	114	-26.9
1971-1980	145	118	-18.6
1981-1985	140	86	-38.5
1986-1990	140	86	-38.5
1991-1995	126	86	-31.7
1996-2000	106	86	-18.89
2001-2005	110	86	-21.8
2006-2010	100	47	-53
2011-2015	92	47	-49
>2015	92	47	-48.9

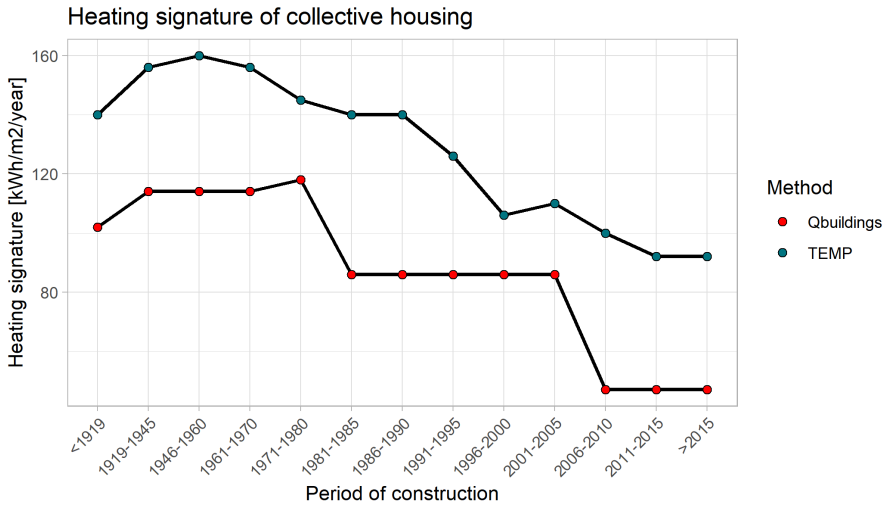

Figure 2.10: Comparison of specific heating needs for a collective housing

Table 2.6: Sierre's annual Hot Watr needs.

	TEMP	Qbuildings	difference
Q^{HW} [GWh/y]	23.9	19.0	- 20 %
q^{HW} [kWh/m^2/y]	14.4	8.8	- 38 %

Hot Water

The difference concerning the Hot Water production is shown is Table 2.6. The density of hot water production q^{HW} differs by 38%. This results from the method applied for evaluating the HW needs. Figure 2.11 illustrates, for a subgroup of buildings, the annual HW demand using different methods. The TEMP employs the Norm 308/1 while *Qbuildings*, which uses a variant of the standard SIA 2024, is lower than SIA 380/1 and SIA 2024. The figure shows that HW needs of three buildings are largely smaller from the value of the SIA 380/1 (- 98 %). It involves the industry and commercial buildings. Then, the individual and collective housing HW needs are respectively 30% and 38% lower than the 380/1 Standard.

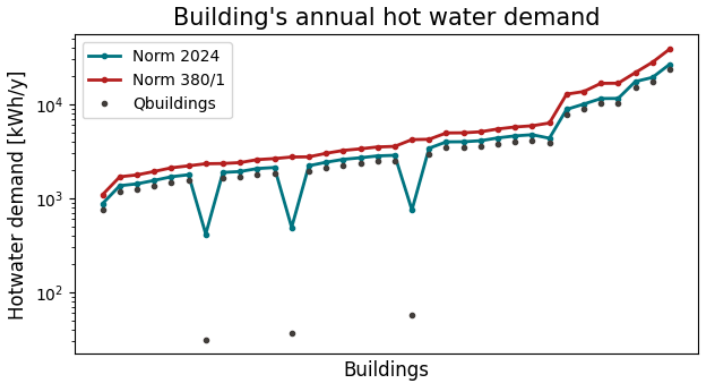

Figure 2.11: Comparison of methods for estimating the Hot Water demand for a subgroup of buildings

2.1.4 Suggested changes to Qbuilding

The comparison between the two methods demonstrates some divergence regarding the assumptions. First, as far as the supply temperature level of heating is concerned (see Figure 2.7), the profile of the TEMP appears to be closer to reality compared to the only two levels proposed by *Qbuildings*. Consequently, for the rest of this study, the three temperature level model (i.e. 70, 55 and 40 °C) will be used in *Qbuildings*.

In addition, the factor f_{gnd} is also highly diverging. Since none of the two studies indicates the source of their assumptions, we have decided to exploit values given by [18] that proceeds to a regression on Swiss buildings data. As described in Table 2.3, [18] provides the factor f_{gnd} in function of the affection of the building. By means of the *Qbuildings* distribution of the affectations presented in

Figure 2.6 and Table 2.3, we reach an average ERA factor f_{gnd} of 0.82. This result also validates the value used by the TEMP and will be in turn employed in *Qbuildings*.

Table 2.7: Value of the ERA factor in function of the building affectation from [18]. The average value is found using the building's affectation given by *Qbuildings* in Figure 2.6

Category	ERA factor f_{gnd}
Individual housing	0.732
Collective housing	0.890
Administrative and commercial	0.787
Agricultural & industrial	0.681
Others	0.702
Average for Sierre	0.820

Concerning the energy signature, the results provided by *Qbuildings* can be considered as an optimistic value in terms of consumption.
Moreover, a significant divergence can be found in terms of The Hot Water demand. In the frame of this study, it has been decided to use the SIA 380/1 standard to estimate the production of Hot Water. This method appears to be more in line with the reality.

Table 2.8: Sierre's annual Space Heating needs.

	TEMP	Adapted Qbuildings	Difference
ERA [m^2]	$1.66 \cdot 10^6$	$1.88 \cdot 10^6$	+ 13 %
q^{HW} [kWh/m^2]	14.4	17.2	+19%
q^{SH} [kWh/m^2]	118.4	94.0	- 20 %
Q^{HW} [GWh]	23.9	32.3	+ 35%
Q^{SH} [GWh]	196.5	176.72	-10.1 %

2.1.5 Validity

The statistical method used to estimate the energy demand is based on many assumptions that are difficult to define. In this chapter, the comparison of the two sources, namely the TEMP and *Qbuildings*, has allowed us to point out critical elements of the analysis, such as ERA factor that is proportional to the final demand. On the one hand, *Qbuildings* only uses open data which introduces the program as applicable to any location. On the other hand, the TEMP exploits a mix of statistics and real data. As a matter of fact, collecting and using real data does provide more precise measurements and values, but concurrently reduces the flexibility of the analysis.

The modification of the assumption linked to the ERA calculation has reduced the ERA difference to 13%. The Sierre's final SH demand amounts to 176.7 GWh per year, which is 10% lower than TEMP's results. Finally, the HW demand amounts to 32.3 GWh/y, corresponding to a value 35% higher than TEMP. It can be noted that the difference in final demand is higher than before the modification made to *Qbuildings*. In fact, previously, the errors were compensated by one another, giving therefore results that appear to be similar.

Now that Sierre's energy demand has been evaluated, it is possible to design the network that will distribute the heat waste from *Novelis* to the city. Next section focuses on the design of a network inside a given district.

2.2 Modelling of the network within a district

In contrary to modern low emission technologies like heat pumps and pv panels, district heating has been existing for almost 150 years. In fact, in 1882, New York installed one of the first steam system to supply the heat to Manhattan [19]. Using heat waste from the industry is a way to provide heat to consumers at a very good price. The heat recovery being very low within the factory, very high temperature waste is released and can easily fulfill the needs of residential districts. The technology became very popular after the oil crisis of 1973 when the price of the barrel went extremely high and especially, in Scandinavian countries. For instance, at that time, Denmark was producing 90% of its energy out of fossil fuels. A large development of district heating completely changed the dependency on fossil fuels: in 2019, 60% of the heat sold in Denmark is produced by DHN [20] [21].

Nowadays, with an upward trend of energy prices and a willingness to cut off the dependence to fossil fuels, the DHN is coming back to the front stage with the same arguments as 150 years ago: low emission, adaptable, safe and convenient for the consumer. Despite that the principle remains unchanged, the technology has significantly evolved.

This section is presenting the challenges of designing a district heating network, by going through different present and future technologies on the market. The methodology to dimension the infrastructure, that is developed in this study, aims to provide an estimation of the price of a DHN based only on the area, the number of buildings and the total power demand of the district. Despite the lack of precision, this method has the advantage of being easily applied to any cities or districts. It gives a first overview of the zones that are more likely to have a DHN installed.

2.2.1 Generations of DHN and importance of temperature level

In the literature, the evolution of DHN is classified into 5 generations. The main element that distinguishes them is the level of temperature. Figure 2.12 shows the characteristics of the different generations. In general terms, the temperature is decreasing for more recent technologies together with an increase of the efficiency. In addition to that, a lower temperature implies that a wider range of heat sources can be exploited. According to [1], the 5 generations of DHN can be described like this:

1st Generation is the oldest version of district heating. The energy is transported under vapour phase, which leads to a high level of thermal losses. Also, the diversity of sources is very limited.

2nd Generation is distinguished by the transition from vapour to pressurized liquid water at a temperature above 100°C, increasing the efficiency compared to the 1G.

3rd Generation allows us to exploit more widely the industry waste by going below the 100°C. The use of renewable energy and industry waste as sources has become more economically viable with this Generation.

4rd Generation aims to lower the temperature as close as possible to the temperature required by the consumers. Energy efficiency and smart integrated energy system are key elements of this evolution. Central heat pumps appears, in this range of temperature, as a good candidate in comparison to the conventional heating plant used in the previous generations

5rd Generation reduces the temperature close to ground temperature. The thermal loss is then almost null. However, a decentralized utility, like a heat pump, has to raise the temperature in function of its end-use. In addition to the high efficiency, the low temperature network can be used for cooling residential buildings and a different type of fluid can be used, like CO_2 [14].

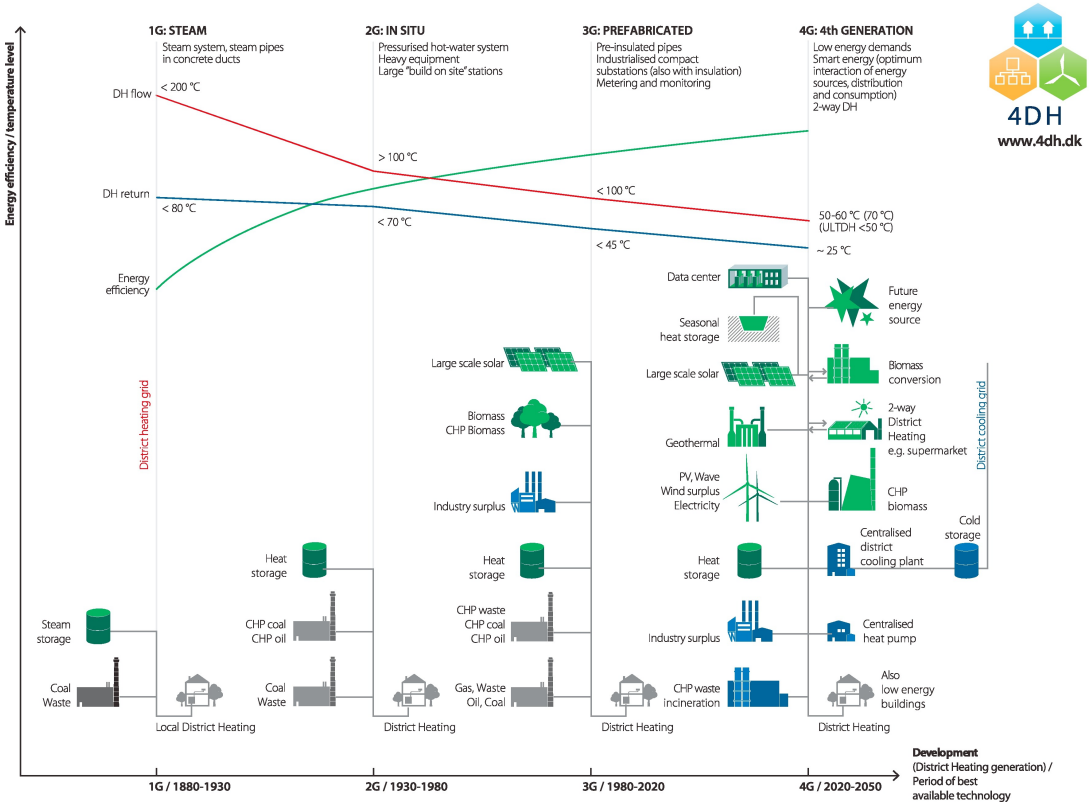

Figure 2.12: Description of the District Heating generations [1]

The system can be modelled as an exchanger whose transmitted heat is described by the equation:

$$\dot{Q}supply = A \cdot U \cdot LMDT \tag{2.11}$$

with $LMDT$, the Logarithmic Mean Difference Temperature of the stream entering and leaving the exchanger. Q_{supply} represents the room's heat demand while U is the heat transfer coefficient and LMDT, the Logarithmic Mean Difference Temperature between the room temperature and the temperature of the supplied hot/cold water. It shows that by increasing the area of the exchanger, the water can be supplied at a temperature closer to the room temperature. This explains the fact that the radiator, whose covered area is smaller than the one of a floor system, requires water to be supplied at a higher temperature.

The exergy losses in a heat exchanger is expressed as:

$$\dot{L}_{HEX} = \dot{Q} \cdot T_a \left(\frac{1}{T_{c,lm}} - \frac{1}{T_{h,lm}} \right) \tag{2.12}$$

This equation illustrates that the exergy losses increase is in accordance with the difference of temperature between both sides. A system with a high efficiency will, then, supply the temperature as close as possible to the room temperature.

To conclude, reducing the temperature of a DHN has the advantage of increasing the exergy and energy efficiency and extending the range of potential heat sources. The main hot spot is the management of the temperature requirement of and for every consumer. For each building that requires high temperature supply, three possibilities can be considered: (i) Do not connect it to the network, (ii) connect it and increase the temperature of the network or (iii) connect the building and compensate the difference of temperature by adding a decentralized heat pump.

2.2.2 Modelling of district network

Now that the different types of DHN have been presented, the development of a model to dimension the network is essential to perform an economic analysis. This section explores the different steps to design the size and length of pipes used in a defined district.
The economical aspect is a determinant success factor of a DEN project. The final price of heat has to be attractive enough for the consumer and at the same time profitable for the investors. The implementation of the infrastructure can take years and the system needs to be running for decades to reach the payback time. One of the main difficulties of developing such a project is that the interest for a consumer to get connected depends on the decision of other consumers. Indeed, the cost of the energy determines whether it is profitable for the consumer, while this same cost varies according to the number of connected buildings.

Mass flow

The energy transferred Q_s from the pipe to the consumer is defined by the enthalpy difference ΔH of the heat transfer fluid between the supply and return pipes:

$$Q_s = \Delta H = \dot{m} \cdot \Delta h \qquad \text{[kJ]} \tag{2.13}$$

The mass flow $\dot{m}$ [kg/s] is given by the amount of heat supplied by the pipe Q_s [kJ] divided by the enthalpy difference of the fluid Δh [kJ/kg]. The enthalpy difference Δh of the fluid corresponds to the sensitive heat for temperature change without phase change and to the latent heat for phase change. In this study, the water DHN is only in water phase while CO_2 is based only on the phase change. Assuming that the temperature difference between the supply T_s and return T_r is constant, the pipe mass flow can be deduced as:

$$\dot{m} = \frac{\dot{Q}_s}{\Delta h} \qquad \text{with} \begin{cases} \Delta h = c_{p,water}(T_s - T_r) & \text{if water} \\ \Delta h = h_{vap,CO_2} & \text{if } CO_2 \end{cases} \tag{2.14}$$

Table 2.9: Maximum liquid velocity in DHN pipes

Pipe Diameter [mm]	Maximum liquid velocity [m/s]
50	1
100	1.4
150	1.6
200	2.1
300	2.5
≥ 500	3

The specific heat of water $c_{p,water}$ is 4.18 $\frac{kJ}{kg \cdot K}$ while the enthalpy of vaporization of CO_2 amounts to 176.65 $\frac{kJ}{kg}$ [3].

Diameter

The price of the infrastructure varies in function of the pipes' diameter. It can be calculated by using the mass flow $\dot{m}$ [kg/s], the flow velocity v [m/s] and the density of the fluid ρ [kg/m^3]:

$$D = \sqrt{\frac{4\dot{m}}{\pi \cdot v \cdot \rho}} \tag{2.15}$$

A higher flow velocity v reduces the required diameter, but increases the friction of the fluid with the pipe wall. It is thus a question of trade off between the price of the pipe and the pressure losses. It has been demonstrated that the best profitability is achieved when the pipes are chosen as small as possible [22]. This range is limited by an admitted maximal velocity, thus avoiding excessive noise and cavitation [22]. The maximum speed velocities employed in this study are taken from [3]. These values, listed in Table 2.9, are used for water DHN but also for the liquid phase of the CO_2 based network. [3] specifies that for the vapour CO_2 phase, the constraints are not the same and that the velocity can be freely chosen. [11] applies a speed of 6 m/s to the vapour CO_2 phase.

Estimation of the pipes length

This section aims to estimate the length of the network within a given district, based on the area and the number of buildings. Girardin [2] assumes that buildings are equidistantly distributed over a given area, as showed in Figure 2.13. Equation 2.16 gives the network route length L for a pair of pipes, in function of the area of the district A, the number of buildings n_b and the shape factor K. The latter is a coefficient that accounts for the street typologies. Since the value of the coefficient given by Girardin [2] is calibrated for Geneva, it is therefore not adapted to Sierre. Section 2.2.4 develops a method to calibrate the coefficient K using the gas grid.

$$L = (n_b - 1)K\sqrt{\frac{A}{n_b}} \tag{2.16}$$

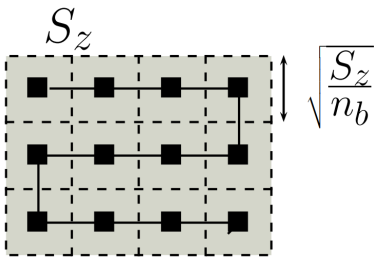

Figure 2.13: representation of the equidistance assumption. From [2]

$$L_k = \frac{L}{n_b} \tag{2.17}$$

Within a district, the diameter gets smaller as the energy is distributed. By assuming that the total demand of the network $\dot{Q}_{tot}$ is equally distributed among the n_b number of buildings of the area (i.e. $\dot{Q}_b = \dot{Q}_{tot}/n_b$), Suciu [11] considers a linear decrease of the mass flow of each section of the network. A section k is defined as the connection between two buildings. The mass flow in the k^{th} section is then given by:

$$\dot{m}_k = \dot{m}_{max} \cdot \frac{n_b - k - 1}{n_b} \qquad \text{with } k = 1, \ldots, n_b \tag{2.18}$$

with $\dot{m}_{max} = \frac{\dot{Q}_{tot}}{\Delta h}$

Finally, the diameter of each section is deduced from (2.15):

$$D_k = \sqrt{\frac{4\dot{m}_k}{\pi \cdot \upsilon \cdot \rho}} \tag{2.19}$$

Water based network piping cost

The investment cost to install pipes includes a fixed cost that accounts for civil engineering works and a variable cost that depends on the diameter of the pipe. Table 2.10 is a synthesis of DHN project conducted in Valais. Concerning the larger diameters, a linear regression of the data is used. Figure 2.14 compares the piping cost of different sources. As shown in Figure 2.14, the cost from Henchoz [3] and Girardin [2] are in average 41% and 52% higher than the data from Valais. In fact, these studies use data from Geneva projects and given the density of the city, the excavation cost is expected to be much higher. The data collected from projects in Valais are then more adapted to the present case study. The cost function can then be written using the parameters c_1 = 4494 CHF/m2, c_2 = 377.8 CHF/m and L the path length of the pair of tubes :

$$C_{pipe} = (c_1 \cdot D + c_2) \cdot L \qquad \text{[CHF]} \tag{2.20}$$

Table 2.10: Cost of insulated pipes for District Heating Network from a synthesis of different studies conducted in Valais. It includes all the civil engineering works, the two tubes (supply and return), including the installation, welding and leak detection.

DN [mm]	25	32	40	50	65	80	100	125	150	200	250	300
Excavation	339	367	367	413	422	431	500	557	573	714	891	986
Pipes (incl. installation)	175	184	194	214	243	270	325	380	422	524	628	782
Total [CHF/m]	514	551	561	627	665	701	825	937	995	1238	1519	1768

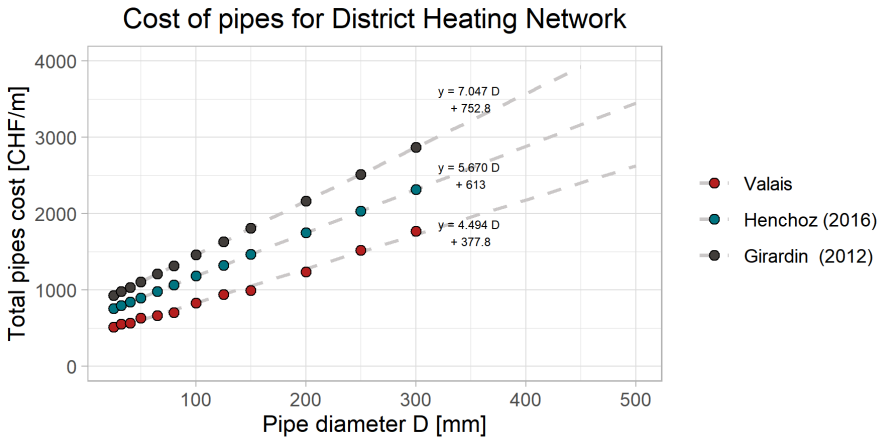

Figure 2.14: Total piping cost including excavation and pipes for supply and return. Data taken from Theses of Henchoz [3] and Girardin [2].

CO_2 based network piping cost

Since CO_2 network is still at the phase of development, the prices cannot be deduced from existing projects. A cost function is however given to estimate the piping cost. Henchoz et al. [14] estimates, in CHF/m, the price of one tube with the following equation:

$$c_{pipe}^{CO_2} = 35 \cdot (D/25)^{\alpha} \qquad \text{with } \alpha \in [0.7, 1.5] \tag{2.21}$$

The cost of excavation is given in [CHF/m] by:

$$c_{excav}^{CO_2} = 1.38 \cdot D + 200 \qquad [\text{CHF/m}] \tag{2.22}$$

Since the vapor phase pipe diameter is larger than the liquid phase, the total cost is written as:

$$C_{pipe}^{CO_2} = \left(35 \cdot \frac{D_{vapor}^{\alpha} + D_{liq}^{\alpha}}{25^{\alpha}} + 1.38 \cdot D_{vapor} + 200\right) \cdot L \qquad [\text{CHF}] \tag{2.23}$$

Figure 2.15 compares the compositions of the cost of water and CO_2 based network. It can be seen that the uncertainty of the CO_2 price is large. For this study, α is set at 1.1. The CO_2 network needs reinforced pipes to support high pressure fluid (50 bars) but, because of the low working temperature (15 °C), the insulation is not required. Then, the excavation cost is smaller for CO_2 network, since it has the advantages of being buried at low depth or under sidewalks [3]. The total cost of pipes installation is shown in Figure 2.16. For diameter smaller than 175 mm, the water pipes are more expensive than the CO_2 one. It is mainly due to the difference in excavation cost that accounts for 3/4 of the water pipes.

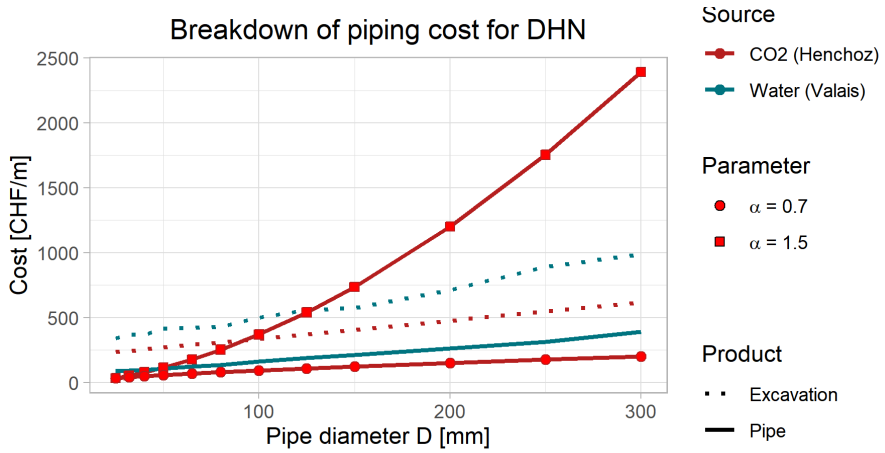

Figure 2.15: Comparison of piping cost between Valais water-based projects (blue lines) and the CO_2 network presented by Henchoz et al. [14] (red line) for the maximum and minimum value of the parameter α.

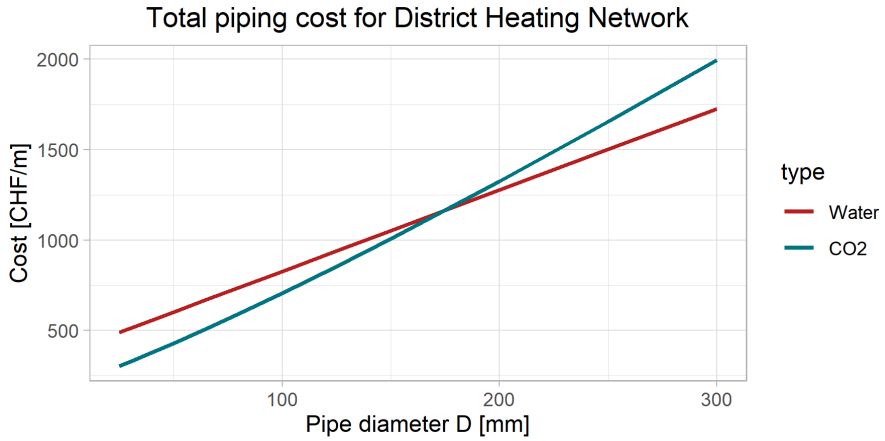

Figure 2.16: Price of the network pipes, including excavation and supply and return pipes

Heat losses

One of the drawbacks of the centralization of the energy production is that losses are occurring when transporting the energy. In the case of a DEN, the energy Q_l is lost by thermal conduction through the walls of pipes. As a consequence, the central plant needs to produce more to compensate the thermal losses. The relation between the heat losses Q_l, the heat demand Q_s and the centralized production Q_p can be expressed by:

$$Q_p = Q_s + Q_l \qquad \text{[kWh]} \tag{2.24}$$

The heat transfer rate between two mediums can be written as:

$$\dot{Q}_s = k_l \cdot A \cdot \Delta T \qquad \text{[W]} \tag{2.25}$$

with k_l the heat transfer coefficient expressed in $\frac{W}{m^2 K}$, A the area exposed to the heat transfer and ΔT the difference of temperature between the two mediums. In the case of a pipe, the heat losses depend on the diameters ($\rightarrow A$), the level of temperature ($\rightarrow \Delta T$) and the quality of the insulation ($\rightarrow k_l$).
[23] models the heat losses of a DHN using the aforementioned parameters. The thermal loss $\dot{Q}_l$ of a two-piped system is described by Equation 2.26 with the diameter D_a, the supply and return temperature T_s, T_r, the network route length for pair of pipes L (1 pipe), the average ground temperature T_{gnd}:

$$\dot{Q}_l = k_l \cdot \pi \cdot D_a \cdot 2L \cdot \left(\frac{1}{2}(T_s + T_r) - T_{gnd} \right) \tag{2.26}$$

The ground temperature T_{gnd} is considered to be 10 °C. An upper and lower bound of the heat transfer coefficient K, expressed in terms of diameter D_a, are defined in [23] as:

$$\begin{aligned} k_{l,low}(D_a) &= 0.7676 \cdot D_a^{-0.341} \qquad \text{[W/m2 K]} \\ k_{l,high}(D_a) &= 0.1088 \cdot D_a^{-0.619} \qquad \text{[W/m2 K]} \end{aligned} \tag{2.27}$$

K_{low} refers to a low quality insulation, while $k_{l,high}$ to high quality and are therefore taken as the upper and lower bound of the losses uncertainty.
In the context of this study, an average quality is considered and can be expressed as:

$$k_{l,medium}(D_a) = 0.4283 \cdot D_a^{-0.4} \qquad \text{[W/m2 K]} \tag{2.28}$$

Figure 2.17 presents the heat transfer coefficient of pipes in function of the diameter of the system and the quality of the insulation. The thermal loss equation can now be deduced using (2.26) and (2.28):

$$\begin{aligned} \dot{Q}_l &= 0.4283 \cdot D_a^{-0.4} \cdot \pi \cdot D_a \cdot 2L \cdot \left(\frac{1}{2}(T_s + T_r) - T_{gnd} \right) \\ &= 2.6911 \cdot D_a^{0.6} \cdot L \cdot \left(\frac{1}{2}(T_s + T_r) - T_{gnd} \right) \end{aligned} \tag{2.29}$$

The relative heat loss in the network is defined as the ratio between the heat loss $\dot{Q}_l$ and the heat injected in the network $\dot{Q}_p$:

$$f_{loss} = \frac{\dot{Q}_l}{\dot{Q}_p} \tag{2.30}$$

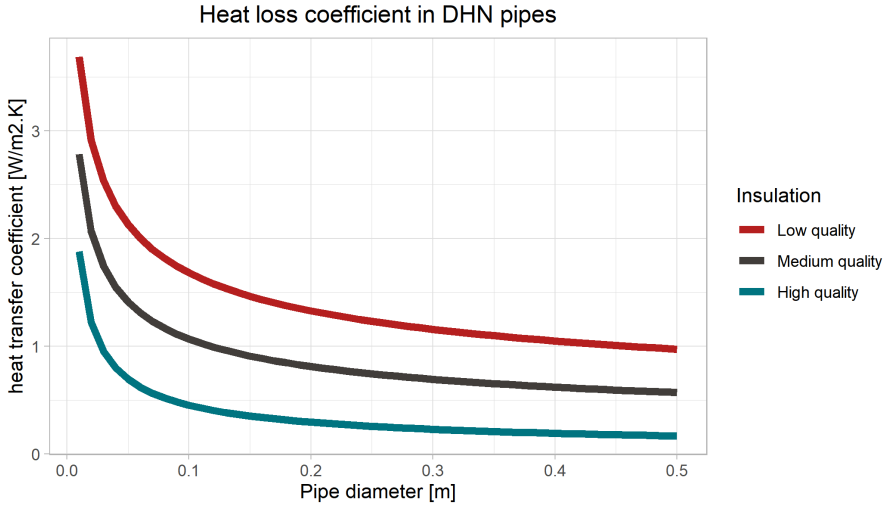

Figure 2.17: Heat transfer coefficient in function of the pipe diameter for three qualities of insulation

In order to compensate the losses, considering that the mass flow $\dot{m}$ and the return temperature T_r are kept constant, the supply temperature leaving the central has to be increased. T_s^* is the corrected supplied temperature. The central has to produce the consumer's needs Q_s plus the losses Q_l. The relation can be written as:

$$\dot{Q}_p = \dot{Q}_s + \dot{Q}_l = \dot{m} c_p (T_s^* - T_r) \tag{2.31}$$

$\dot{Q}_l$ is given by Equation 2.29 with the corrected supply temperature T_s^*

$$\begin{aligned} \dot{Q}_s &= \dot{m} c_p \Delta T - \dot{Q}_l \\ &= \dot{m} c_p (T_s^* - T_r) - 2\pi k_l D_a L \left(\frac{1}{2}(T_s^* + T_r) - T_{amb} \right) \\ &= \dot{m} c_p T_s^* - \dot{m} c_p T_r - \pi k_l D_a L \cdot T_s - \pi k_l D_a L \cdot T_r + 2\pi k_l D_a L \cdot T_a \\ &= T_s^* (\dot{m} c_p - \pi k_l D_a L) - T_r (\dot{m} c_p + \pi k_l D_a L) + 2\pi k_l D_a L \cdot T_a \end{aligned} \tag{2.32}$$

The corrected temperature of supply T_s^* can be finally written in function of the heat rate demand $\dot{Q}_s$:

$$T_s^* = \frac{\dot{Q}_s + T_r (\dot{m} c_p + \pi k_l D_a L) - 2\pi k_l D_a L \cdot T_a}{\dot{m} c_p - \pi k_l D_a L} \tag{2.33}$$

2.2.3 Definition of districts

When this methodology is used in a case study, the districts' boundaries need to be determined. There are different ways to do it, as for instance: meshing, clustering algorithm, manual design, etc. In order to have a model that can be adapted to any cities, the manual district definition is not the

most suitable method. In the context of the case study of Sierre, it has been decided to use a mesh to split the city into equal areas. Squared and hexagonal mesh of different size are compared. Figure 2.18 illustrates examples of mesh used to define districts.

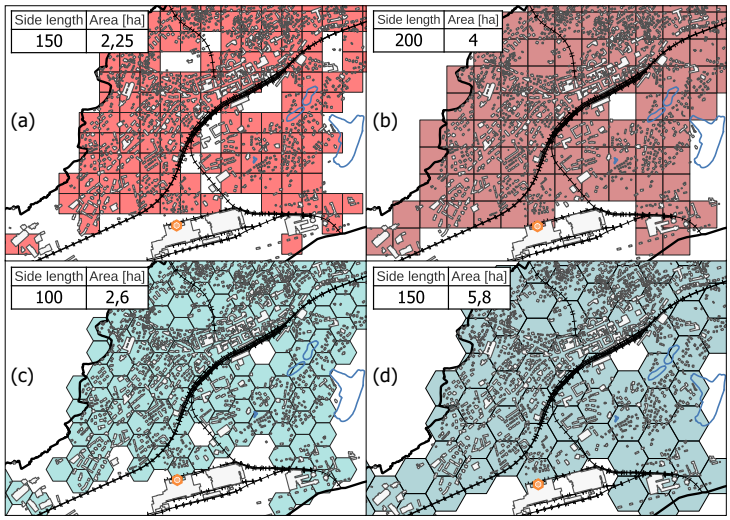

Figure 2.18: District definition using a mesh. The size of the district is determined by the side length of the geometry.

It can be noted that a district can also be designed by grouping the buildings connected to the same medium-low voltage transformer. It has the advantage of defining district that are optimized for the distribution of electricity. In the same way, it would also be adapted for heat distribution. However, the data were not available for the present case study.

2.2.4 Calibration of shape factor K

Equation 2.16 gives an estimation of the piping length L in a given district in function of the shape factor K. [2] determines the value of the coefficient using the existing infrastructure of Geneva. For the case of Sierre, since the density and the architecture are different, a calibration of the factor is preferred. The gas network, whose path is optimized as it would be done for a DHN, is taken as reference. The goal is to optimize the constant K with the aim to minimize the error between the estimation length L and the gas grid length.
Figure 2.19 presents the absolute error of the total network length in function of the shape factor K and for different sizes and type of districts. It shows that the value of K converge between 0.406 and 0.496 and the absolute error does not significantly differ. It is then suggested to choose the grid that fits the best the studied city. In the present case study, the hexagonal grid of size 150 is chosen.
For each district, the relative error between the estimated length and the gas grid length is illustrated in Figure 2.20. It can be underlined that the error is lower than 6% for districts with a high number of buildings. Naturally, the shape factor should vary according to the type of district (e.g. city center, high density residential area, low density residential area,...). However, some districts have a low ratio of buildings connected to the gas network, which distorts the calibration of the DHN length. Figure

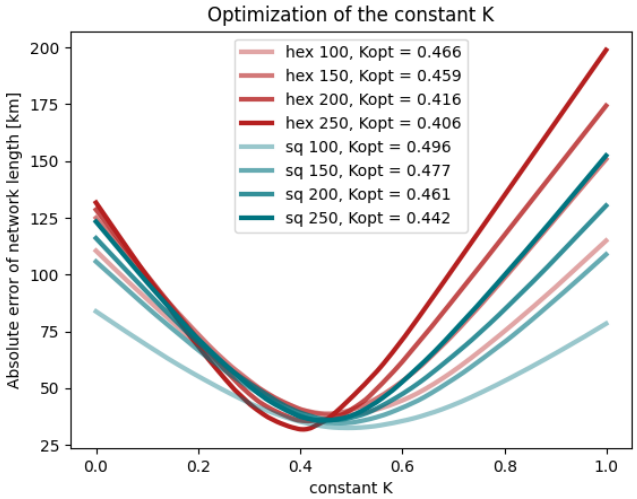

Figure 2.19: Absolute error of the network length estimation

2.21 illustrates this point. In fact, the right district has a low accuracy since the gas network is not widely developed, which alters the estimation. On the other hand, the left district estimates well the network length. For this reason, it is preferred to calibrate a unique shape factor K for the entire city.

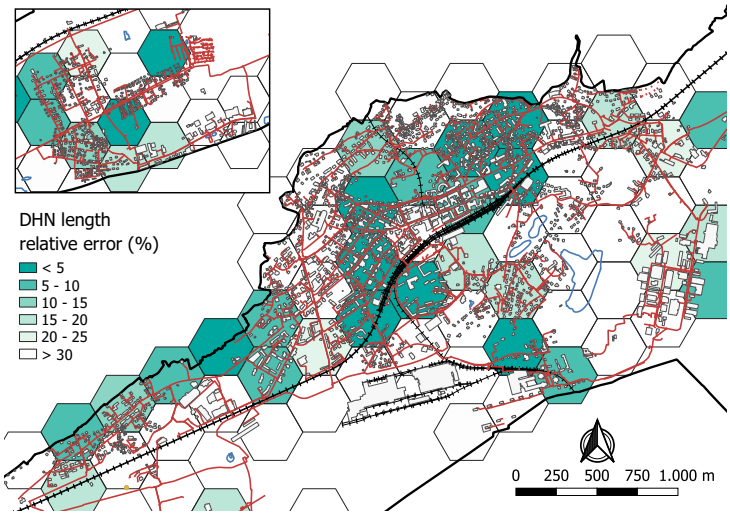

Figure 2.20: DHN length estimation relative error compared to gas grid length. The orange lines represent the gas network

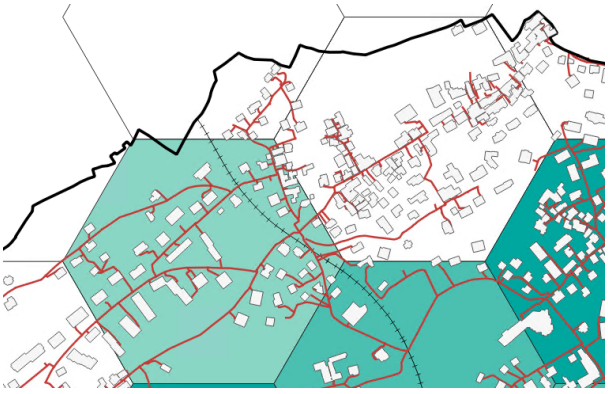

Figure 2.21: Zoom in Figure 2.20 to highlight limits of this method.

Up to this point, we have defined the energy demand of the city (Section 2.1), delimitated the districts (2.2.3) and estimated the infrastructure cost to connect every building to a network (Section 2.2.2). The cost of DHN infrastructure of each district of Sierre can then be calculated and is represented in Figure 2.22. As expected, districts with high density and energy demand, like the city center, have a lower pipes investment cost.Therefore, it results in a good overview of the most attractive zones of Sierre.

The next section focuses on selecting and connecting a certain number of districts to the heat source by minimizing the cost of the system.

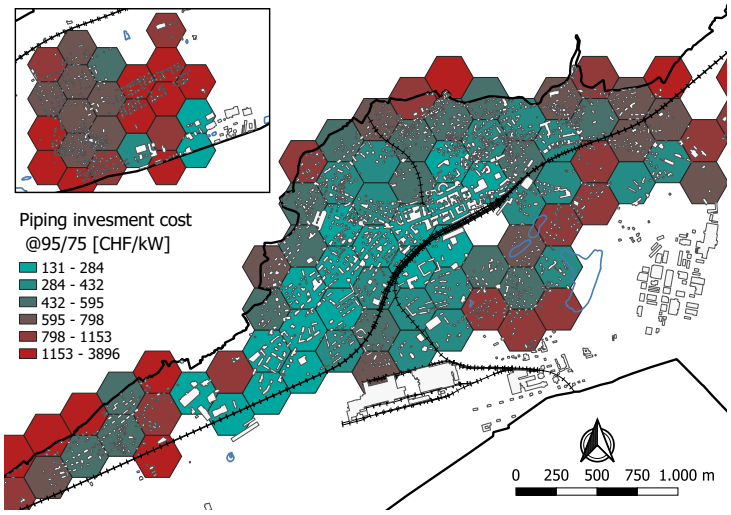

Figure 2.22: Map of the piping cost for a 95/75 °C network.

2.3 Optimization of the district network for industry heat waste recovery

Up to now, the cost of the infrastructure for a district has been estimated with the help of the equidistant assumption. For each sector of the city, a specific piping cost is computed. Now that the demand and the distribution have been evaluated, the energy source needs to be addressed. This chapter focuses mainly on recovering the heat released by the aluminium factory *Novelis* located on the territory. A strategy will be developed to the select the optimal set of districts that will be connected to the industry. Afterwards, the path that links all the selected districts is determined by using the graph theory.

2.3.1 Districts rating

It is complex to define the optimal selection of districts to be connected to the network, since many parameters need to be taken into consideration. A brute force method could be used by generating all the possible combinations of districts. However, the number of combinations is extremely high, thus implying a high computational time. The methodology used in this study consists in reducing the number of sets by rating the districts. Then, only the n top-ranked ones are connected to the heat source. Different criteria are selected to evaluate the potential. The first one is the infrastructure cost c_Q related to the energy supplied in CHF/kWh. Secondly, the districts with high annual heat demand Q are more likely to be connected to the network. Finally, the distance to the source $dist$ influences the cost of connection : it is preferred to connect buildings close to the industry. A normalized grade, related to each of the three criteria, is attributed to every district: G^{c_Q}, G^Q and G^{dist}. Facing the difficulty to attribute a relative importance between the three grade, a weight w is added. The final grade of the k^{th} district is given by:

$$G_k = G_k^{c_Q} + w^Q \cdot G_k^Q + w^{dist} \cdot G_k^{dist} \tag{2.34}$$

The weighting factors are employed to generate alternative solutions. Figure 2.23 displays the grade for the districts of Sierre with the weights w^{dist} and w^Q set to 1. In this configuration, the city centre is the region with the highest grade. A high energy density as well as a relatively short distance to the factory make these districts of interest.

2.3.2 Type of thermal network

Many possibilities exist when it comes to the design of the district energy network. The decision is based on parameters such as the type of sources, the size of the network, the type of consumer, etc. As presented in Figure 2.24, three basic types of thermal networks can be distinguished: *radial*, *looped* and *meshed* grid. The radial network has the advantage to have the shortest route to connect all buildings and is easier to model. On the other side, the lopped and meshed designs allow us to integrate more than one energy source. In addition, despite the increase of investment cost, these networks promote the security of supply and the extensibility. They are then preferred for a larger

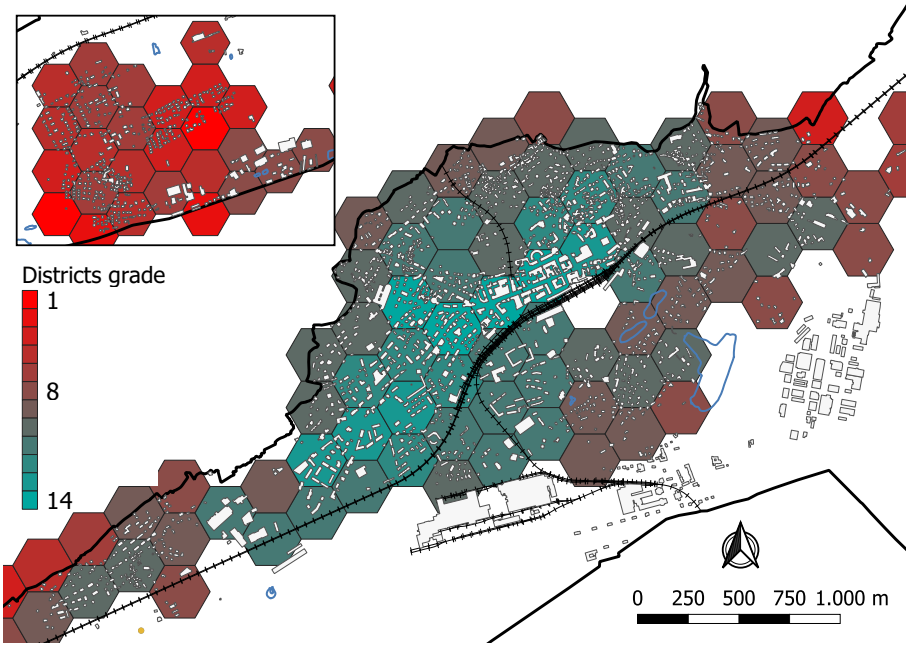

Figure 2.23: Grading of Sierre's districts. The weights w_{dist} and w_Q are set to 1. An increase of the distance factor w_{dist} would favor districts closer to *Novelis*

network. [4]

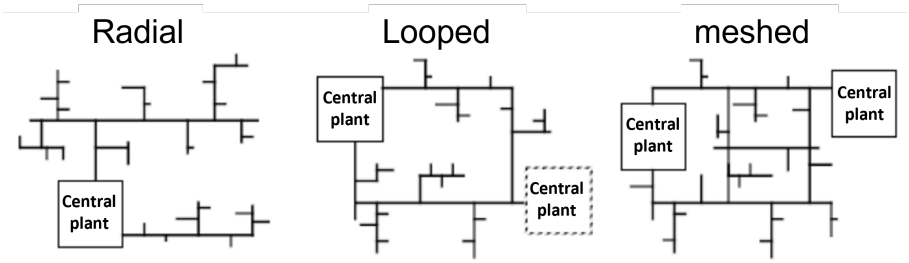

Figure 2.24: Representation of basic types of thermal networks. Figure adapted from [4]

Within the context of this study, the *radial* design is selected. This choice is motivated by the fact that the case study only considers one heat source (i.e. *Novelis*) and that the absence of loops reduces the complexity of the model.

Since the energy demand is not constant over the year, auxiliary utilities could be required for the peak demand. It is then considered that this difference is compensated only by one utility located directly on the source's site. Moreover, a closed system with two pipes is taken in account. This difference of temperature of the two pipes allows the consumers to extract the heat or, in specific cases, evacuate the heat through the network. Figure 2.25 illustrates the model that is examined in this study. The cost of pipes inside the district is evaluated in Section 2.2.2 while this section focuses on evaluating the cost of the connection pipes (blue lines).

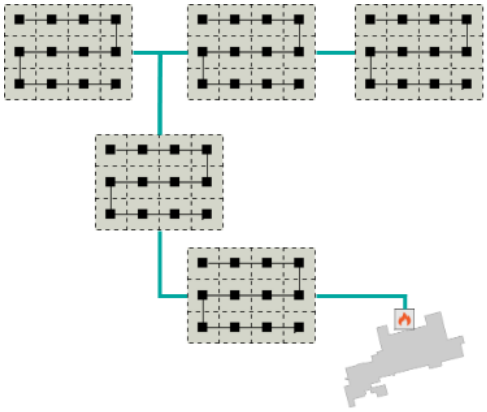

Figure 2.25: Representation of the districts' connection to the source. The total cost of the infrastructure takes into consideration the connection pipes between the districts (blue lines) and the network inside each district (black lines). The industry, in grey, releases its waste to the network. The auxiliary unit, illustrated by the flame, is located on site.

2.3.3 Linear connection

In section 2.3.1, the most interesting districts have been identified. It is now possible to define the path that the network will take to connect all the districts to the industry. For that purpose, the Minimum Spanning Tree (MST) is computed. As illustrated in Figure 2.26, it represents the set of edges that links all the points together by minimizing the sum of the edge weights. Kruskal's algorithm enables us to compute the MST with a complexity of $O(m \log n)$. The algorithm needs as input, a matrix M_{MST} that indicates the weight of each combination of points. In the present case, the weight associated to the edges are the direct distance between each point.

Figure 2.27(c) presents the optimal piping path to connect the 15 best ranked districts using the Minimum Spanning Tree algorithm. The connection piping length amounts to 3940 meters. Although the computation time is low, the main issue of this method is the fact that the path crosses obstacles, like buildings or railways.

2.3.4 Routing

In order to further the network path design, it is possible to describe in more details the path of pipes. In fact, with the methodology presented in Section 2.3.3, the districts are connected with straight lines which cannot be applied in reality. It would be more realistic to follow the roads. The MST methods could be exploited by using, in the distance matrix, the shortest route rather than the straight line distance. The python API of *Open Street Map* (OSM) allows us to obtain the shortest route to connect two geographic points. The used python library is named *OSMnx* [1].

This methodology can be applied in two different ways:

[1] https://osmnx.readthedocs.io/en/stable/

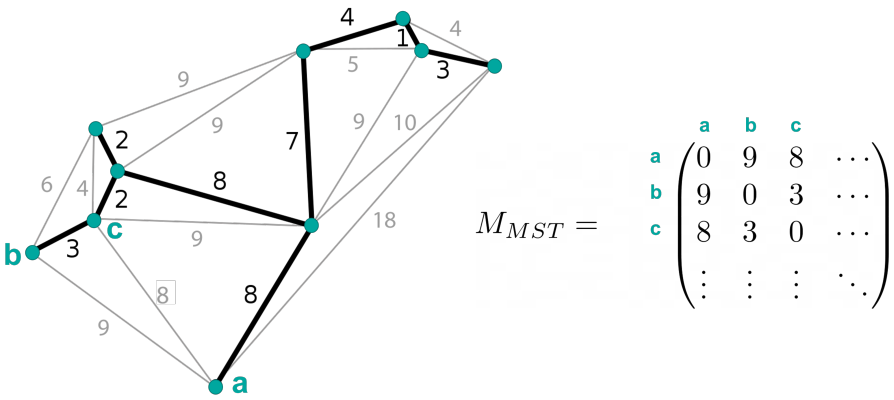

Figure 2.26: Representation of the distance matrix of a graph.

(a) **Post-MST routing**: Compute the linear MST to determine the connections. In a second phase, use the navigation service to find the shortest path between each connected district.

(b) **Pre-MST routing**: Calculate the MST by using a modified weight matrix M_{MST}: the weights are, in this case, the shortest distance using road instead of direct distance.

2.3.5 Comparison of network design methods

Figure 2.27 shows the network designed by the three methods. The linear method (c) has the lowest computation time, but produces a result that is not very realistic since obstacles are not taken into account.
Figure 2.27(a) computes the shortest path after the optimization of the Minimum Spanning Tree (MST). The piping length has increased by 70% with respect to the linear solution of Figure 2.27a. However, as it can be seen in the figure, the solution is still not optimal: the shortest direct distance does not necessarily lead to the shortest route.
Therefore, the optimization of the MST needs to be processed by taking into consideration the road distance and not the direct distance. The Figure 2.27(b) shows that this route is more efficient: the connection length goes down to 5360 m. The computation time is higher since the shortest path needs to be found for all combinations of districts in order to fill in the weight matrix M_{MST}.

It can be noted that when the routing is used, the geometry of the road is imported from the *OSMnx* library. By indicating the name of the concerned city/region, the library automatically imports the right data. This process may take about 10 seconds, which explains the high computation time of Figure 2.27 (a) and (b). It is however possible to locally save the map in order to avoid this importation time.

Another advantage of saving the map locally is that it can be manually modified. In fact, when designing a DHN, external constraints can appear regarding the path of the pipes. The graph can be then modified on a software (e.g. *Qgis*) to delete a road that cannot be exploited in reality or on the other

hand, to add extra pathways. Figure 2.28 shows an example of this manual modification. On the original solution, two redundancies can be observed. The one on top of the figure is due to the fact that the graph for walk routing takes into account sidewalks on both sides of the road.

It can also be noted that, when a navigation system is used to connect two points, it is possible to select the type of transportation (i.e. walk, bike or car), which affects the optimal path. According to the results, *walk* optimization is the mode that is the most appropriate for this purpose. In fact, *bike* and *car* options can be restricted by one way roads which could cause a deviation and by the fact that they cannot access pathways reserved for pedestrians.

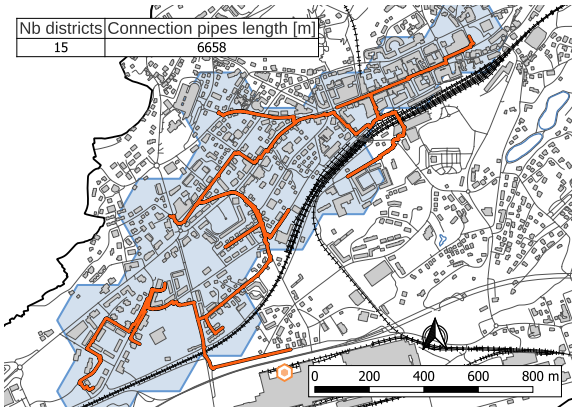

(a) Post-MST routing
Computation time: 20 s

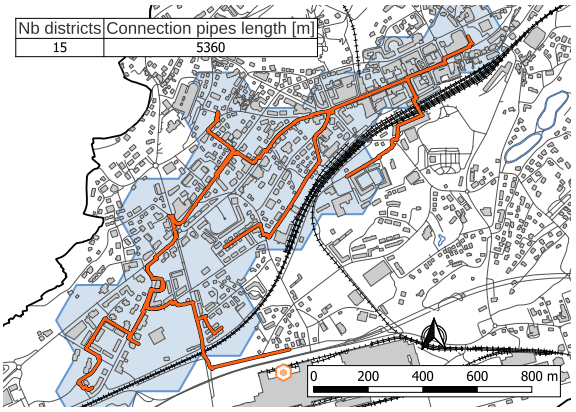

(b) Pre-MST routing
Computation time: 25 s

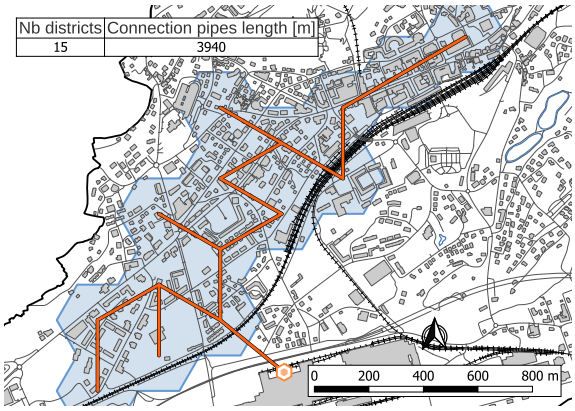

(c) Linear connection optimization.
Computation time: 5 s

Figure 2.27: Results of the Minimum Spanning Tree for network design. OSM navigation service is used either before generating the MST (a) and post MST (b). Two methodologies to connect the 15 districts (highlighted in pink) to the source by minimizing the total piping length. The heat source is indicated by the orange dot.

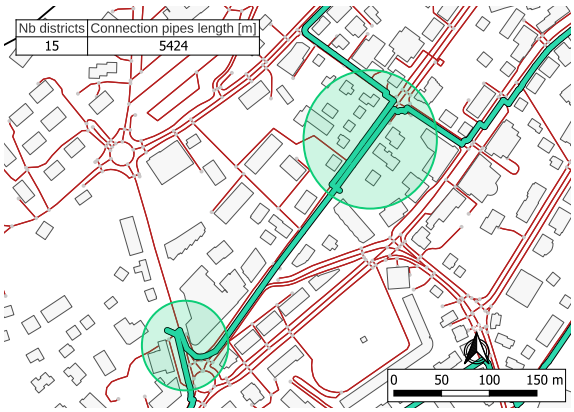

(a) Original solution

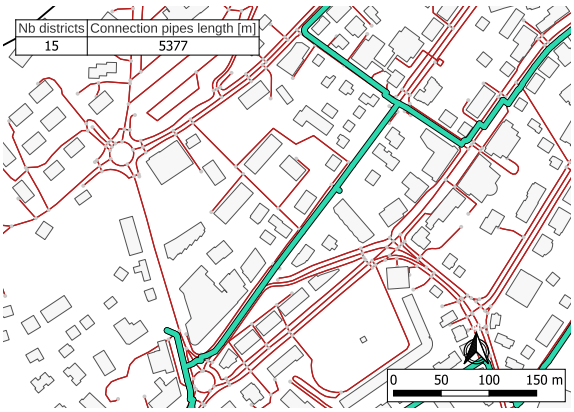

(b) Solution after manual modification of the road graph

Figure 2.28: Improvement of the solution by manually modifying the road graph. The red lines are the graph imported from the library and the blue line the DHN pathway solution. Lines of the graph are deleted in (b) to avoid inconsistency.

2.3.6 Total infrastructure cost

As it was presented previously, the cost of piping depends on the provided heat power and the temperature of the heat transfer fluid. Water with higher temperature difference demands a lower mass flow, which results in a lower pipe diameter. Once the route taken by the network is calculated, the total cost of the infrastructure can be estimated by means of the following equation :

$$C_p = \sum_{i}^{N_d} C_{p,i}^{d} + C_p^c \qquad \text{[CHF]} \tag{2.35}$$

The total cost of piping C_p consists of the sum of the network investment $C_{p,i}^{d}$ of each district i, and of the connection cost C_p^c that links the N_d districts to the centralized energy source.
By assuming that the cost of the infrastructure is distributed equally over the districts, the energy price induced by the piping investment can then be deduced by:

$$\tilde{C}_Q = \frac{\tilde{C}_p}{Q_{SH} + Q_{HW}} \qquad \text{[CHF/(kWh·y)]} \tag{2.36}$$

with $\tilde{C}_Q$ and $\tilde{C}_p$ the annualized costs with an interest rate of 5% and a lifespan of 60 years.

2.3.7 Generation of alternative solution

Now that the infrastructure cost of a solution can be deduced, we have to be sure that the best configuration is selected. As explained in Section 2.3.1, the district grading is computed by setting two weighting factor w^Q and w^{dist}. By varying these weights, the ranking is changing and the selected districts are then different. Every combination of weight yields to a new solution of DHN. Figure 2.29 shows an example of economical comparison of DHN solutions. Every point represents a solution, i.e. a set of districts connected to the central plant. The solutions are generated by varying the weights

w^Q and w^{dist} and the number of connected districts. The piping cost is expressed in CHF/kWh according to equations (2.35) and (2.36). Depending on the amount of energy that it is intended to be delivered, the solution should be taken within the red line, in order to minimize the cost.
Figure 2.30 illustrates the cost of the optimal solution for three level of temperature. With a reduced diameter, the CO_2 DHN has the lowest cost of the four temperature level.

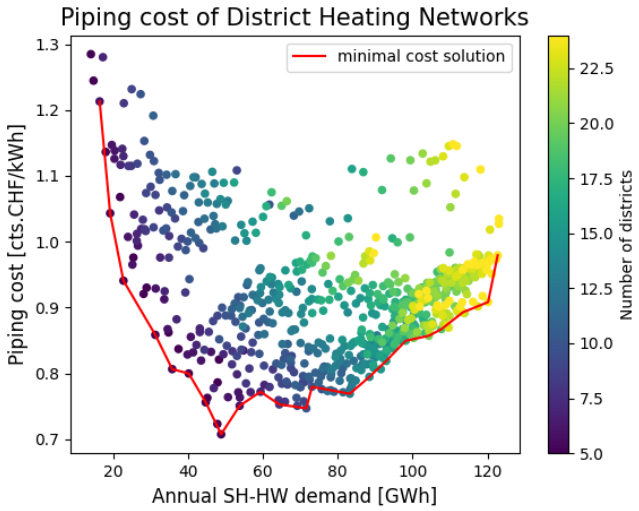

Figure 2.29: DHN piping cost for a supply/return temperature of 95/75 °C. The X-axis indicates the annual heat distributed for Hot Water (HW) and Space Heating (SH). Each point represents a configuration of districts.

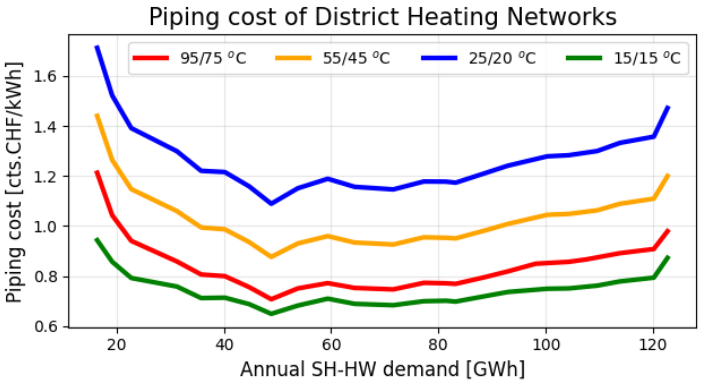

Figure 2.30: Comparison of the annualized cost of pipes for different level of temperature.

2.3.8 Design of auxiliary unit at central plant

In contrast to the industry, the heat demand of a city is not constant over the year. In order to determine the amount of heat that can be recovered, the energy profile needs to be analysed. Figure 2.31 shows the heat rate demand $\dot{Q}^{HW+SH}$ profile of a group of districts and points out the lack of

power during winter. On the contrary, during summer, the industrial heat can not be recovered by the city and then has to be dissipated in another way.

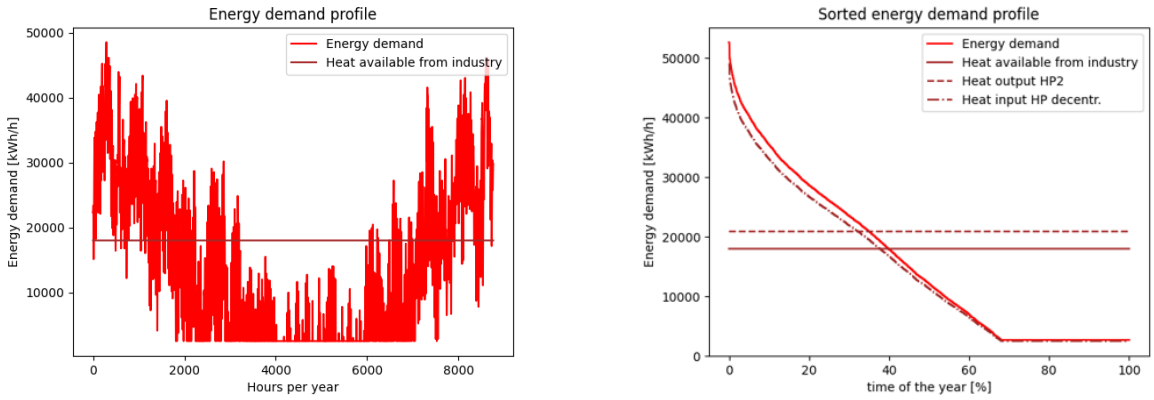

(a) (b)

Figure 2.31: Heat demand profile (SH and HW) of 25 districts connected to the 55/45 °C DHN. The dark red line shows the heat available provided by the industry. The dashed line is the power available after the heat pump has increased the temperature level of the heat waste. The dashed dotted line is the heat required at the input of the decentralized heat pump.

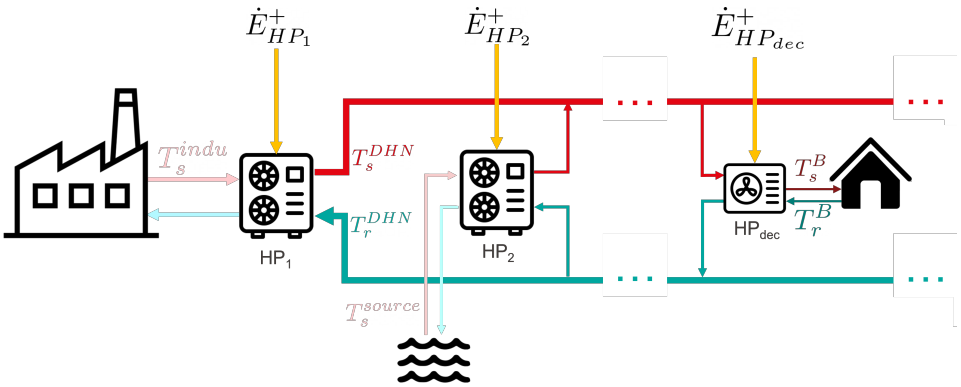

Figure 2.32: Scheme of the auxiliary unit of the DHN

As it was mentioned earlier, a DHN can have more than one central plant, especially in large looped or meshed networks (see Figure 2.24). In the present case, the radial network with one central plant is considered. In addition to being a low emission technology, heat pumps have a high efficiency (COP) when using heat waste. For this reason, this technology is considered in this study.

Figure 2.32 presents the system modelled in this study. The central plant is composed of two heat pumps. The first heat pump (HP1) has the role of upgrading the temperature level of the source to the temperature level of the DHN. The second heat pump (HP2) compensates when the industry heat rate is not sufficient, especially during very cold days. Finally, the decentralized heat pump (HP_{dec}), located in the consumer building, is used to increase the temperature of the DHN to the

building requirement temperature. The use or not of these three types of heat pumps depends on the type of DHN and on the heat supplied by the industry. In order to design the auxiliary utilities, the following parameters are required:

- T_s^{DHN} : The supply temperature of the district network
- T_{indu} : The temperature of the industry's heat waste
- $\dot{Q}_{indu}^{+}$: The annual profile of the heat flow provided by the industry
- $\dot{Q}_s$: The annual heat demand profile

Temperature level upgrade (HP1)

The utility needed to increase the temperature of the source is used when the network working temperature is not reached. Using a carnot factor ε of 0.55, the COP of the heat pump is given by:

$$COP_{HP_1} = \frac{T_s^{DHN}}{T_s^{DHN} - T_{indu}} \cdot \varepsilon \tag{2.37}$$

The heat rate $\dot{Q}_{HP}^{-}$ (Equation (2.39)) is the energy supplied by the heat pump after the temperature level upgrade. It is computed by using the energy balance and the COP definition. Figure 2.31(b) shows, in dashed line, the corrected heat available after the temperature level upgrade.

$$\dot{Q}_{HP_1}^{-} = \dot{E}_{HP_1}^{+} + \dot{Q}_{indu}^{+} = \frac{\dot{Q}_{HP_1}^{-}}{COP_{HP_1}} + \dot{Q}_{indu}^{+} \tag{2.38}$$

$$\iff \dot{Q}_{HP_1}^{-} = \frac{\dot{Q}_{indu}^{+}}{1 - \frac{1}{COP_{HP_1}}} \tag{2.39}$$

The size of the heat pump is given by the input electric power:

$$\dot{E}_{HP_1}^{+} = \frac{\dot{Q}_{indu}^{+}}{COP_{HP_1} - 1} \tag{2.40}$$

The total energy produced by the first heat pump $Q_{HP_1}^{-}$ corresponds to the area A in Figure 2.33. This allows us to compute the annual electricity consumption of the heat pump:

$$E_{HP_1}^{+} = \frac{Q_{HP_1}^{-}}{COP} \tag{2.41}$$

Decentralized heat pump

This utility is used when the temperature of the network is lower than the temperature required by the buildings. The COP can be computed as:

$$COP_{HP_{dec}} = \frac{T_s^{build}}{T_s^{build} - T_s^{DHN}} \cdot \varepsilon \tag{2.42}$$

with T_s^{build} the temperature required by the building.

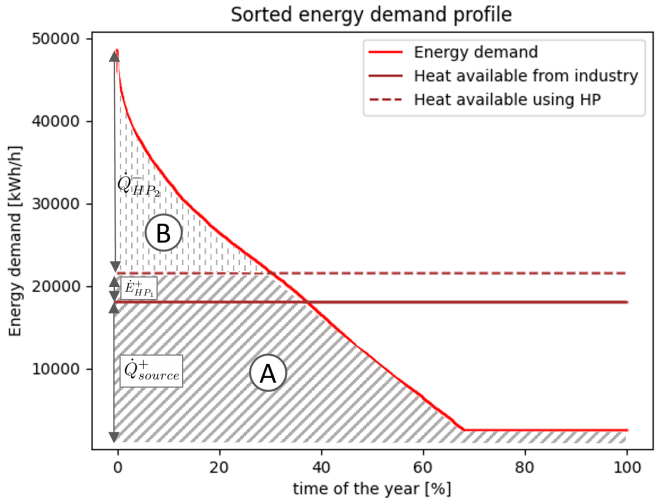

Figure 2.33: Distribution of the energy production between the industry source and the second heat pump. The A area is the energy delivered by the first heat pump. B represents the energy compensated by the second heat pump

The COP enables us to deduce the heat input of the decentralized heat pump $Q^{+}_{HP_{dec}}$. In other words, it corresponds to the heat that needs to be transported by the DHN:

$$\dot{Q}^{+}_{HP_{dec}} = \dot{Q}_s \cdot (1 - \frac{1}{COP_{HP_{dec}}}) \tag{2.43}$$

Heat Pump 2

The second heat pump has the role to complete the heat production for reaching the required heat power. The auxiliary heat corresponds to the area B in Figure 2.33. The utility should be able to produce a heat rate $\dot{Q}^{-}_{HP_2}$ in order to reach the power requiered by the decentralized heat pump. The thermal losses are also taken into account:

$$\dot{Q}^{-}_{HP_2} = Q^{+}_{HP_{dec}} + \dot{Q}_l - \dot{Q}^{-}_{HP_1} \tag{2.44}$$

The size of the utility $\dot{E}^{+}_{HP_2}$ is given by the electric power that depends on the COP:

$$\dot{E}^{+}_{HP_2} = \frac{\dot{Q}^{-}_{HP_2}}{COP_{HP_2}} \tag{2.45}$$

$$COP_{HP_2} = \frac{T_s^{DHN}}{T_s^{DHN} - T_{source}} \cdot \varepsilon \tag{2.46}$$

Now that the size of the heat pumps is determined, it is possible to compute the investment cost. In addition to that, the HPs' electricity profile is used to deduce the operating cost. The Sankey diagram in Figure 2.34 shows the energy flow of a 55/45 °C network.

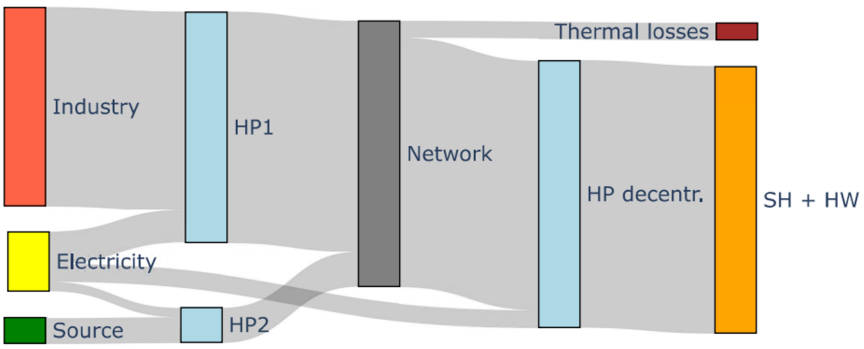

Figure 2.34: Sankey diagram of the 55/45 °C network

Table 2.11: Economic characterisation of the central heat pump.

	c_2^{inv} [CHF]	c_1^{inv} [CHF/kWe]	unit	life [year]	Source
Central Plant heat pump	43020	891	kWe	20	[24]

Chapter 3

Results

The choice of the energy system of a building depends on many factors, such as energy cost, emission and other external elements. The level of emission of a system is often inversely correlated to the investment cost, making the decision complex to take. This chapter explores and analyses the different scenarios and solutions that could be imagined for Sierre to recover the heat from *Novelis*.

3.1 Definition of the scenarios

As it has been shown all along this study, many parameters are involved in the design of a District Heating Network. For this purpose, we consider different scenarios that implement a configuration of network.
In the frame of this study, the industry *Novelis* plans to evacuate the leftover heat with the aim that the city can recover it. After the optimization of the industrial processes of the aluminium factory, the temperature of the released heat will be relatively low, but still difficult to predict. For this case study, we assumed a heat waste temperature of 30 °C and supplied at a constant power of 18 MW.

Four levels of temperature are considered in this analysis and refer to the 4th and 5th generation of District Heating. First, a 95/75 °C network has the advantage of supplying heat to the buildings without the need of a decentralized utility. As seen in Section 2.1, the maximum temperature required by the buildings is 70°C. A temperature difference of 5K is then guaranteed at the consumer's exchanger. Then, a 55/45 °C scenario illustrates the case where the decentralized utility is only needed in non-recent buildings. Finally, the 5th generation is presented by two anegry scenarios : 25/20 °C water based network, close to the industry temperature level and a CO_2 network working at a unique temperature of 15 °C.
Finally, it is assumed that the second heat pump uses the water of Rhône as heat source. The temperature of the water is set to 7.5 °C.
The four temperature levels are then:

- High Temperature network: 95-75 °C

- Medium Temperature network: 55-45 °C
- Anergy water based network : 25-20 °C
- Anergy CO_2 network : 15-15 °C

3.2 Geographic analysis

As developed in the Methodology chapter, the districts connected to the network are chosen on the basis of a grading system. Then, the path of the pipes is generated using a routing optimization. This section aims to present the results of the district selection and of the optimized path.

Figure 3.1 presents the evolution of the network expansion. First, Figure 3.1(a) shows that the covered surface expands from two high energy density zones: the city center (north) and the Rossfeld area (southwest) which is composed of large commercial sector and collective housing. Case (b) extends to the shopping center zone (bottom left) and to the hospital (upper part of the map). In 3.1(c), the three separate areas meet each other and the residential area located south of the station is connected. The last step of the expansion (d) now includes lower density residential area in the northern part of the city.

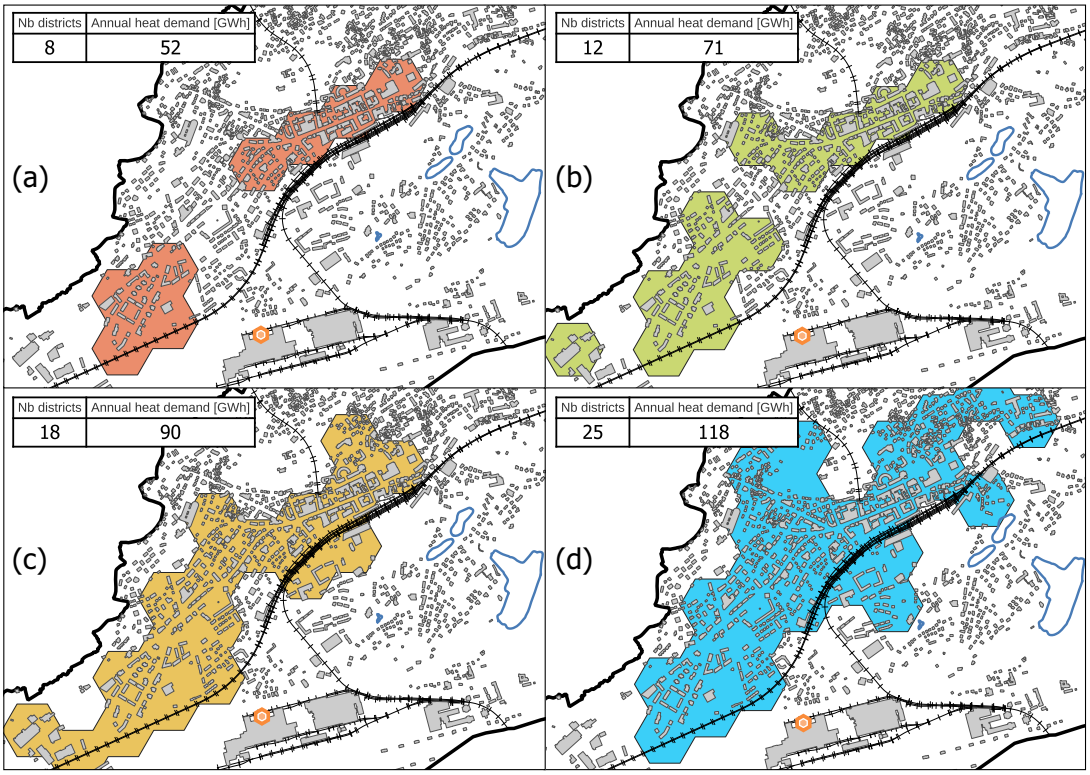

Figure 3.1: The maps present the four scenarios of network expansion for the case study. These networks represent respectively 21%, 30%, 38% and 50% of the total city heat demand.

Concerning the path of the network, Figure 3.2 presents the route for connecting the 17 best ranked districts. The route is generated using the methodology presented in Section 2.3.4. The pipes that connect the districts together (connection pipes shown in Figure 3.2) have a total length of 5732 m while the piping length inside the districts for connecting buildings (not displayed in Figure 3.2) amounts to 10509 m with a maximal diameter of 200 mm.
The path suggests connecting the city to *Novelis* by the west side of the territory. In fact, the railway line limits the possibilities to enter the city.

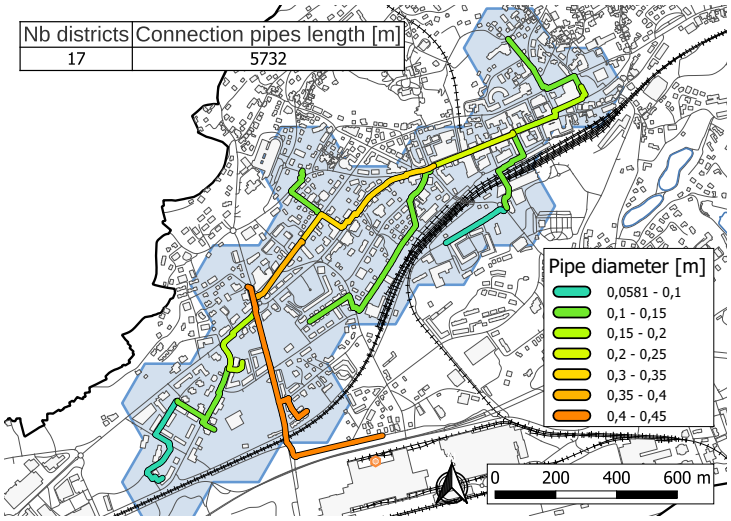

Figure 3.2: Path of the pipes network for connecting the 17 districts generated using MST optimization and routing method.

3.3 Technical results

Unlike the heat rate of the industry that remains constant, the consumer heat demand varies all along the year and may need an auxiliary unit if the industry power is not sufficient. As presented in Section 2.3.8, the model considers that three types of heat pumps can be installed in the system, depending on the size and type of districts. Figure 3.3 shows the power distribution among the different sources. For all cases, the total power increases in function of the size of the network. The red area, that represents the heat waste industry, increases until reaching the limit available (here 18 MW). At this point, the second HP (orange area) is installed as a complement.
For (c) and (d), the temperature of the DHN is not sufficient to directly supply the consumers, hence a decentralized heat pump is installed in every building (grey area) and accounts, respectively for (c) and (d), for 21% and 25% of the total power. On the other hand, (b) can supply the most recent buildings (whose temperature requirement is 40 °C) without the need of a decentralized utility. As a reminder of section 2.1.3, the 40 °C buildings represents 12% of the total ERA of Sierre. The need of decentralized heat pumps is then reduced in comparison to (b) and contributes to 6% of the power. Finally, (a) uses a level of temperature that is sufficient to cover the needs of all buildings without any

decentralized unit.

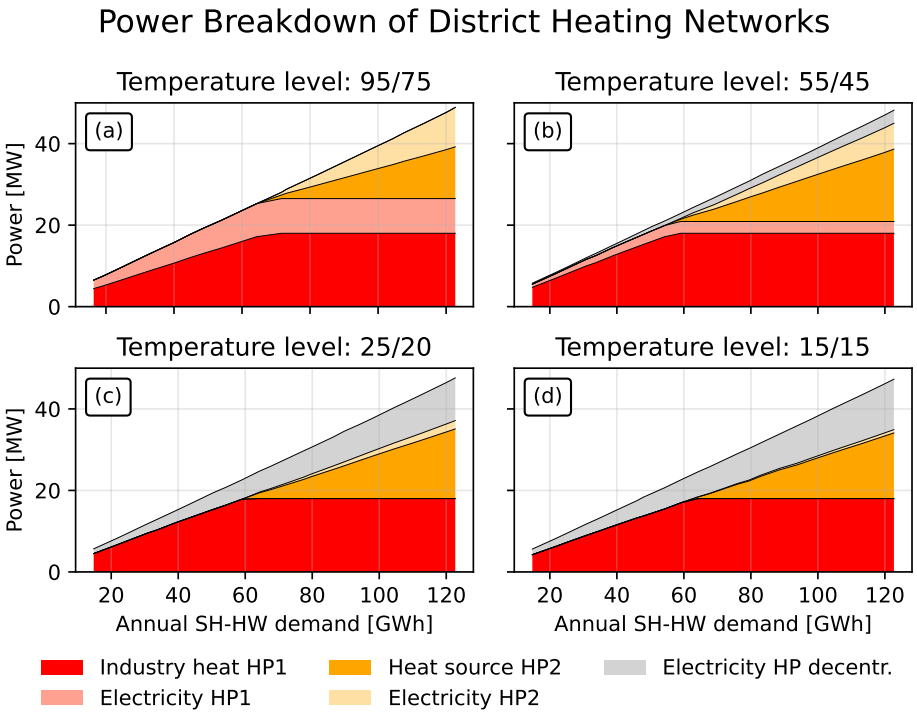

Figure 3.3: Breakdown of the power delivered in function of the size of the DHN.

The breakdown of the energy, shown in Figure 3.4, is different compared to the power breakdown. In fact, the second HP, which only operates during the high demand period, produces only a small share of the total demand. For example, depending on the temperature level, at 100 GWh, HP2 provides 27% to 40% of the power, while only 3% to 7% of the annual energy. The contribution of the HP2 is the highest for the 55/45 °C network, which has a capacity factor of 5.6 %. On the other hand, the 95/75 °C network uses the second heat at only 3.5 % of its maximal capacity. The contribution of the decentralized heat pumps in terms of energy is respectively from the highest to the lowest temperature level 0%, 5.1%, 21% and 25%.

Since *Novelis'* heat waste is limited, the energy provided by renewable sources decreases with the size of the network. This indicator can be measured using the global COP of the system. It is calculated by dividing the total heat demand by the total electricity consumed by heat pumps. Figure 3.5 shows the evolution of the global COP according to the size of the network. The 55/45 configuration has the best COP among the four temperature levels, with a peak value at 6.2 which corresponds to a rate 84% of energy coming from renewable heat (industrial or environmental heat). It is explained by the minimization of the temperature difference across the heat pumps. The high temperature network (95/75 °C) has, by far, the lowest global COP : the rate of renewable heat goes down to 65%. In fact, the heat pumps have to rise the temperature from 30 °C (HP1) and 7.5 °C (HP2) to 95 °C which implies a low COP compared to the other configuration. The descending trade of the COP can also be noted.

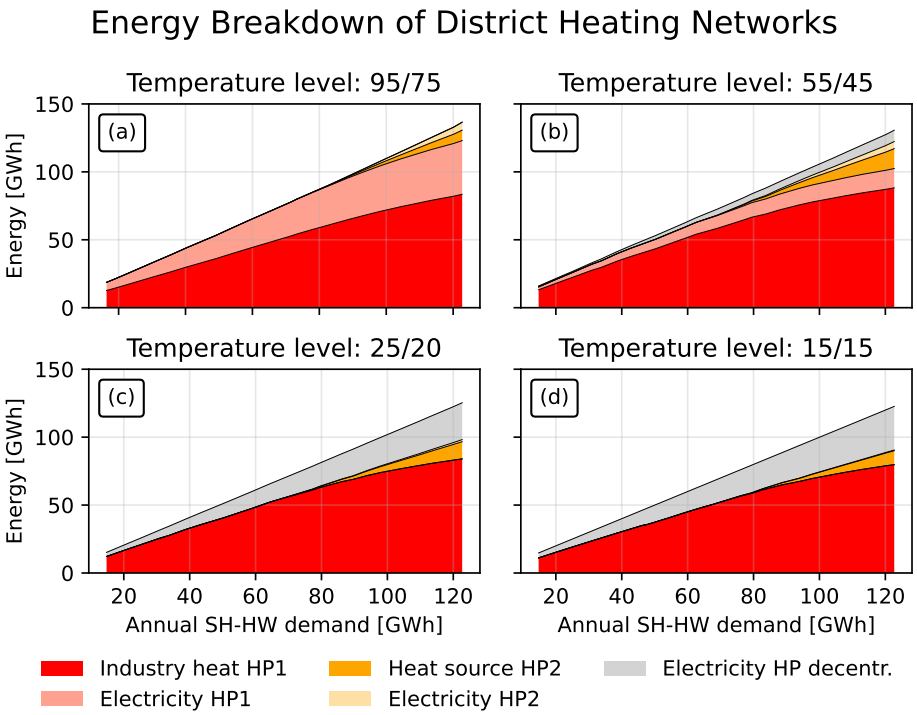

Figure 3.4: Breakdown of the energy production of the four levels of temperature in function of the size of the DHN.

In fact, within a larger network, the share of the energy produced by the HP2 is increased. Since the COP of this second utility is lower (heat source at 7.5 °C vs. 30 °C for HP1), the global COP is affected. A higher efficiency of the system is then achieved with a reduced size of network.

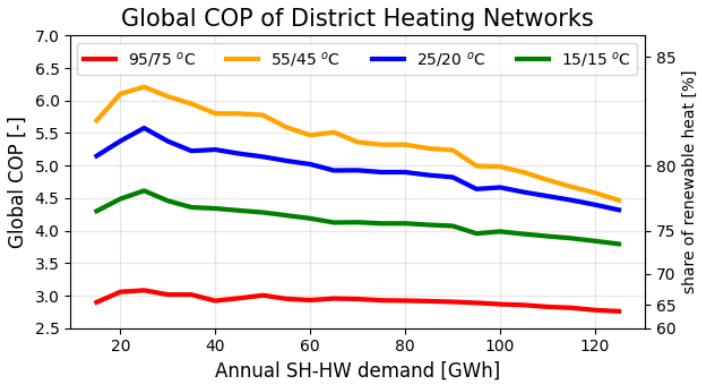

Figure 3.5: Global COP of the system in function of the size of the network for different level of temperature.

The reduction of the share of energy supplied by the industry is shown in Figure 3.6. On the other hand, increasing the scope of the network allows us to recover a larger share of the heat released by *Novelis*. The energy that cannot be recycled by the city needs to be evacuated in another way, which

implies extra investments. It is then important to take into consideration this indicator. Figure 3.6 shows that up to 50% of the industrial heat can be recovered by the city to cover around 50% of its total needs. It can be highlighted that, in this case, the share of the needs covered by the DHN varies similarly to the share of *Novelis*' heat recovered.

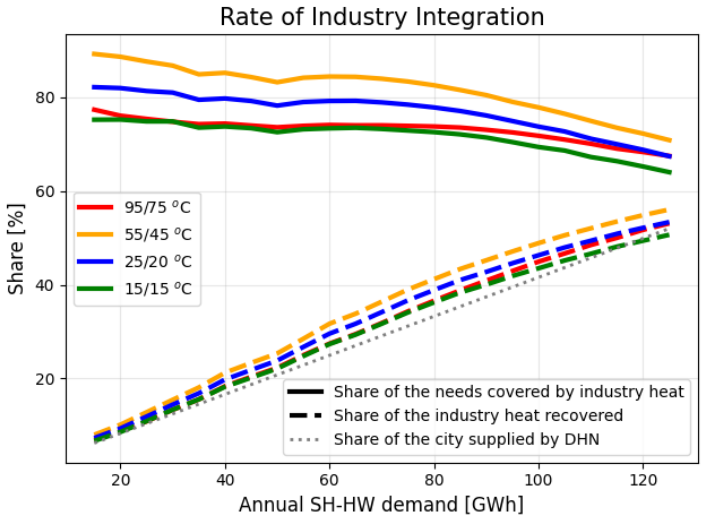

Figure 3.6: Rate of industry integration in the city. It shows the share of the industry heat that is recovered by the city in function of the size of the network.

In addition to the heat supplied by the industry, electricity is required to run the heat pumps, which increases the city's electric consumption. Figure 3.7 shows the electric consumption due to the operation of the network. For the same size of district, the 95/75 °C configuration consumes 33% to 64% more electricity than the CO_2 network and 63% to 114% more than the 55/45 °C network. With a network that supplies 120 GWh (50% of the city demand), the electric consumption of the city increases by 61% with 55/45 °C, 63% with 25/20 °C, 72% with 15/15 °C and is doubled (+100 %) with the 95/75 °C network.

3.4 Economical and Environmental analysis

Reducing the carbon footprint of the city's heating system is one of the main motivation of implementing a district heating network. The performance in terms of CO_2 avoidance is assessed by comparing the emission of the actual case to the one after installation of the network. The accounted emissions concern here only the operation of the heating utility, namely the combustion of fossil fuels or the emission embedded in the consumed. The **RegBL** database provides the type of heating system used in the city's buildings. This allows us to make an estimation of Sierre's present emission. 70 % of the needs are covered by natural gas, 16% by heating oil, 6% by electric heater, 3% by wood and 2% by heat pumps. Since the networks reviewed in this study are driven by heat pumps, the emissions are only linked to the electric consumption. The emissions linked to the electric mix of

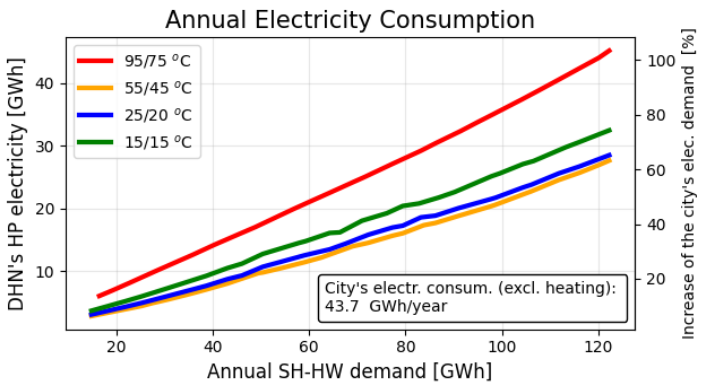

Figure 3.7: DHN electric consumption in function of the heat delivered and increase rate of the total city electric consumption.

OIKEN amounts to 22.27 g CO2-eq.[25] [26]
Figure 3.8 presents the global warming potential (GWP) reduction of the districts connected to the DHN. These emissions are only linked to the concerned area by the DHN and not to the entire city. It shows that the emissions, in Carbon dioxide equivalent, is reduced by 92 to 95% depending on the level of temperature. The difference of emission between the temperature level is due to the value of the COPs that impacts the electric consumption. The 55/45 scenario has the lowest impact, which can be explained by the fact that the global COP of the system is higher. On the other hand, the 95/75 consumes a large amount of electricity because of the low COP of the first heat pump.

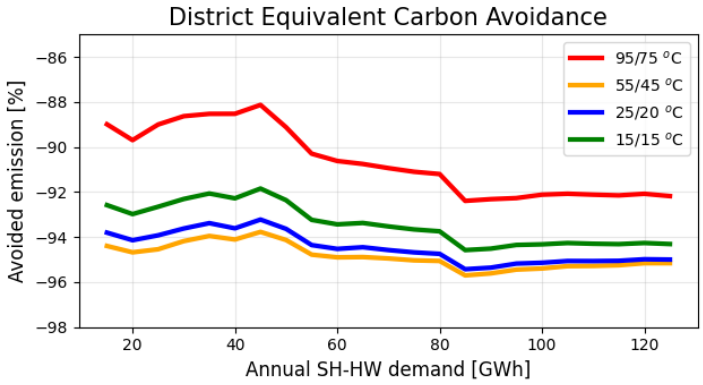

Figure 3.8: Avoided heating emissions in the area connected by the DHN in function of the size of the network. The DHN allows us to reduce the equivalent CO_2 emissions by 88% to 96%.

Figure 3.9 shows a comparison of the heating emissions for the entire city in function of the expansion of the network. With a network that supplies 120 GWh/year (corresponds to 50% of the city's demand), the heating emission can be lowered by 55% to 58%. It can be explained by the fact that the districts with high density, like the city center, are more likely to use fossil fuels than individual housing districts, where heat pumps are more frequent.

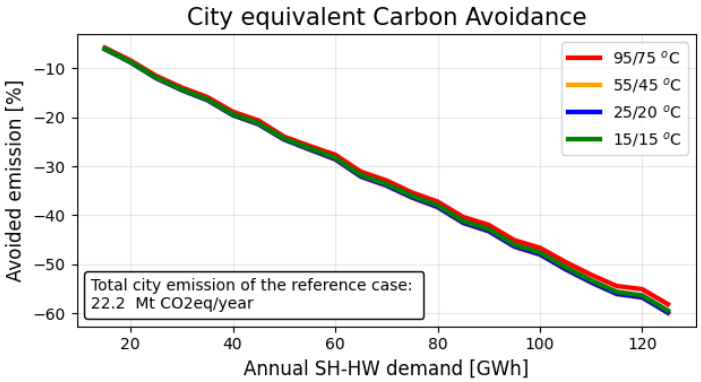

Figure 3.9: Reduction of the city's equivalent CO_2 emission linked to heat production.

The integration is then an efficient solution to decarbonize the heating system of the city. However, the final cost of energy is the determining element that assesses the feasibility of the project. Figure 3.10 shows the distribution of the investment cost in function of the size of the network and of the temperature level. In general terms, the trend is the same regardless of the spread of the network. With a larger pipe's diameter, the 25/20 configuration has the highest piping investment, but is also, in total, 16% to 25% more expensive than the CO_2 network and 58% to 72% than the 95/75 one. The 55/45 configuration is the only one that requires the 3 types of heat pumps, leading to a large infrastructure. However, the excellent COP of this solution enables us to reduce the size of the utility and implies a limited investment in heat pumps.
The high temperature network (95/75 °C) represents the lower investment cost. In fact, a reduced cost of pipes, due to the smaller required diameter and the absence of decentralized heat pumps, results in a total investment cost 36% to 42% lower than the second less expensive solution, namely 55/45°C network.
The CO_2 solution requires the lowest piping investment cost: the reduced excavation cost and the small diameter of pipes are the advantages of this solution. The network cost is 1% to 12% lower than the 95/75 configuration and 37% to 43% than the anergy water based one. However, the decentralized investment cost is important, making the configuration more expensive than the conventional DHN.

As it has been presented previously, the global COP of the system varies in function of the size and type of DHN. The COP determines the electric consumption of the heat pumps, thus the operating cost (OPEX) of the system. Figure 3.11 now illustrates the operating cost of the DHNs expressed in CHF per kWh of heat supplied to the consumer. In the same way as for the investment costs, the trend is the same for any size of DHN. However, the high temperature configuration (95/75 °C) is currently the most expensive to operate and reaches 7 cts.CHF/kWh. In fact, the low temperature provided by *Novelis* implies an intensive use of the first heat pump to reach the required temperature (low COP). It represents an expense 63% to 93% higher than the less expensive network, namely 55/45 °C.
The CO_2 network OPEX is almost entirely composed of decentralized heat pumps. With a temperature of 15 °C, the decentralized heat pumps have a lower COP than the 25/20 or 55/45 networks,

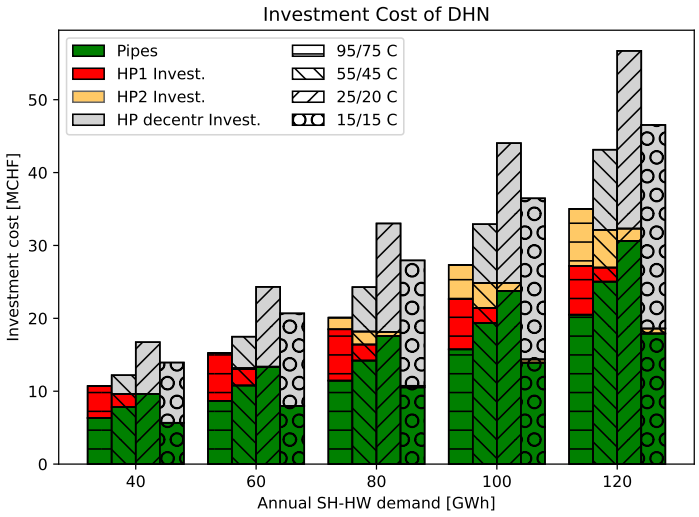

Figure 3.10: Breakdown of the DHN investment cost.

leading to a higher consumption of electricity.
The second heat pump, which has the role of compensating what cannot be supplied by the industry, represents only a small part of the operating cost while the investment cost of this second heat pump can, in some cases, be higher than HP1 (Figure 3.10). It is explained by the fact that the second heat pump is only used part of the time, while HP1 is constantly running.

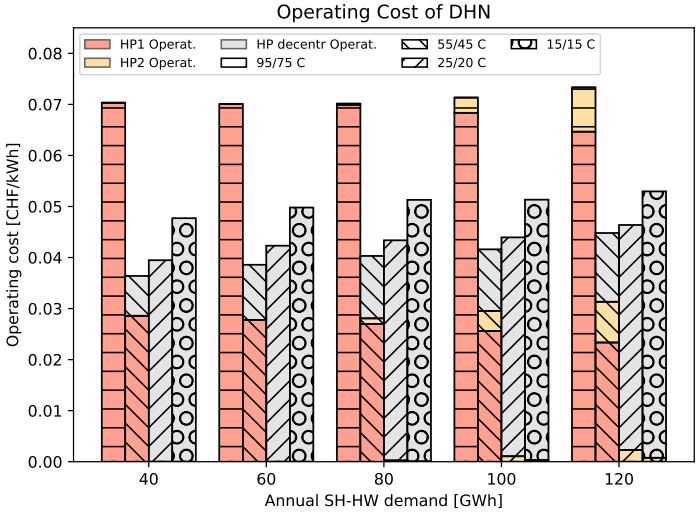

Figure 3.11: Breakdown of the DHN operation cost.

In order to compute the total cost of the network, the investment costs need to be annualized. In the context of this study, a service life of 20 years for heat pumps and 60 years for the network infrastructure is assumed. The interest rate is set to 5%. The distribution of the cost of energy is shown in Figure 3.12. The cost is expressed in CHF per unit of heat provided to the consumer. In a general way, the network becomes more expensive with extreme size, i.e too small or too large.

Configuration (a) is, for any network size, the most expensive solution. The minimum price, that occurs at a network size of 47.8 GWh, is 56% higher than (b)'s and 19% than (d)'s. Moreover, the operating cost of the HP1 represents, at this minimum point, 81% of the total energy price.
The 55/45 scenario is the cheapest among the four temperature levels with a price of 5.5 cts.CHF/kWh. (c) and (d), that reach the minimum cost at the same size, are respectively 22% and 31% more expensive. A linear regression of the cost helps to express the marginal cost of the DHN. From the minimum cost, (b), (c) and (d) have a marginal cost of respectively 0.16 cts.CHF/10GWh, 0.11 cts.CHF/10GWh and 0.8 cts.CHF/10GWh. The CO_2 based network is then the least sensitive to the increase of the DHN size.
The configuration that minimizes the price is shown in Figure 3.13(a) for the 55/45°C, 25/20°C and 15/15°C system, and in Figure 3.13(b) for the 95/75 °C network. The connected districts in Figure 3.13(a) have a high rate of buildings that require medium and low temperature, which both increase the global COP and thus reduce the expenses linked to the decentralized heat pumps.

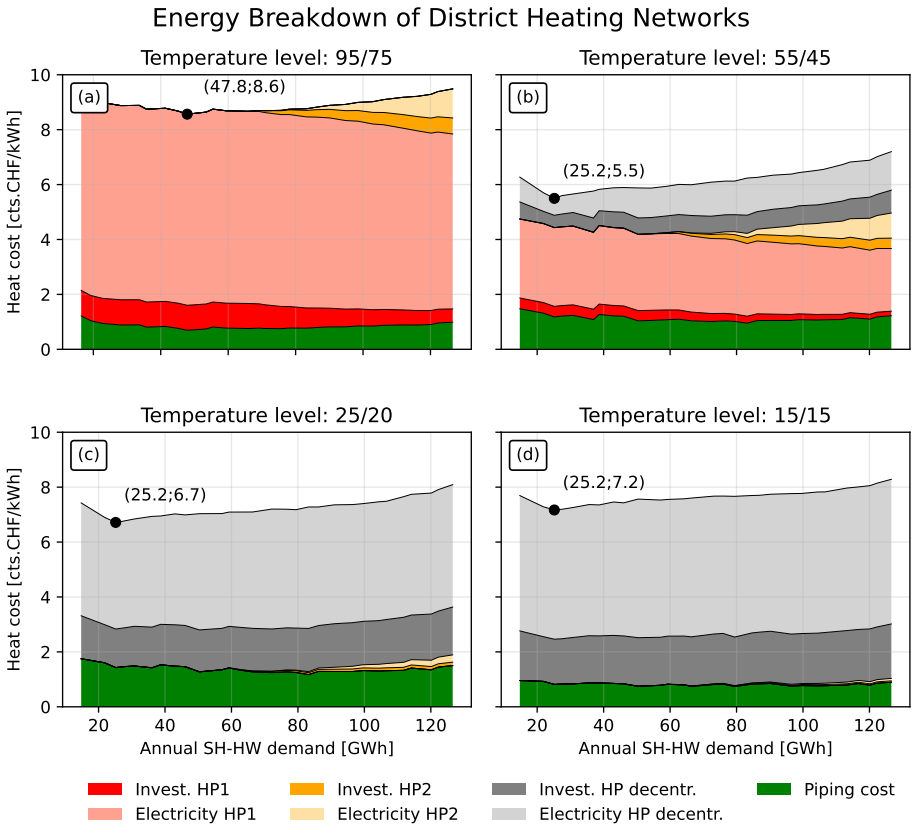

Figure 3.12: Breakdown of the heat cost delivered by the DHN.

3.5 Sensitivity of the Industrial heat waste temperature

The temperature and the heat waste released by the *Novelis* depend on the optimization of the factory and is then highly uncertain. However, the previous results use a fixed industrial temperature of 30

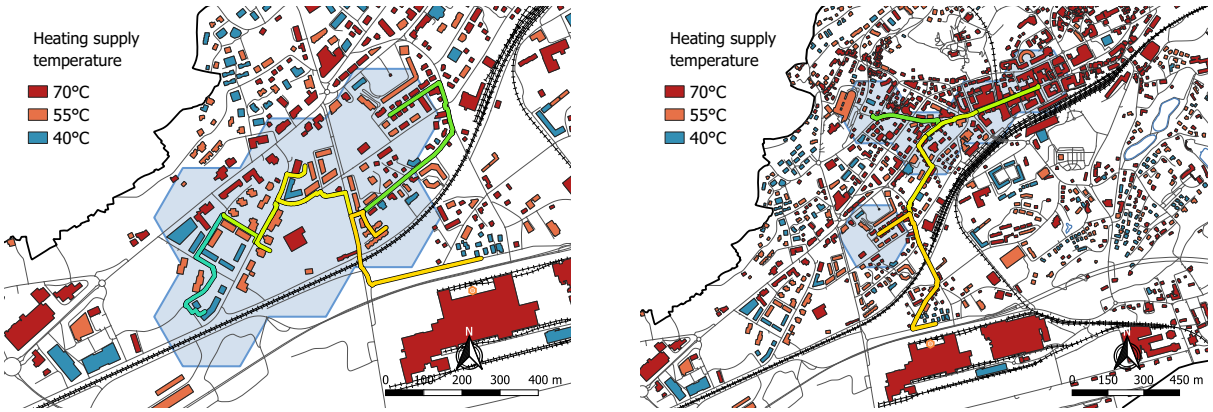

(a) Temperature level: 55/45°C, 25/20°C and 15/15°C

(b) Temperature level: 95/75°C

Figure 3.13: Configuration of the DHN that minimizes the final cost. (a) is a configuration that has a particularly low global COP since a high rate of buildings requires medium or low temperature. The configuration is then specially cost-effective for the DHN equipped with decentralized heat pumps.

°C. This section aims to assess the impact of *Novelis*' temperature on the system. The optimization is processed on the system with a range of waste temperature from 70 to 20 °C. Figure 3.14 compares the final heat cost of the four types of network with different waste heat temperatures T_{indu}. First, it can be noted that as long as T_{indu} is larger than the DHN supply temperature, the cost does not vary with T_{indu}. From an exergetic point of view, this temperature difference should be minimized. Once the T_{indu} is lower than the network working temperature, an auxiliary unit is required, implying an increase of the heat cost. For example, with T_{indu} from 70 to 30 °C, the price of the 95/75 °C configuration is increasing while the price of the water anergy and CO_2 network stays constant.
The CO_2 network becomes more attractive than the water-based anergy one when the available heat is down to 20°C. The 55/45 °C system is the technology that remains the most cost-effective within this range of T_{indu}. It is however only 2% to 3% cheaper than 25/20°C and 15/15°C system.

3.6 User interface

The methodology presented in the study is implemented in a python project. The goal is to generate the design of a District Heating Network that connects a city to a heat source, like industry or water treatment plant. The program aims to be as flexible as possible, meaning that it has been conceived in order to be easily adapted to any cities/region. The main required input are the results of *Qbuildings*. To be more precise, this consists of a *GeoPackage* file containing the localization of all buildings as well as their energetic signature. Then, the heat source is characterized by a location, an annual available heat and its temperature.
The first step of the program is to generate a grid to form the districts. The user is able to select the shape and the size of the meshing. Then, in function of the number of districts that the user wants to connect, the temperature level of the network, the type of fluid and the weighting factors (see Section

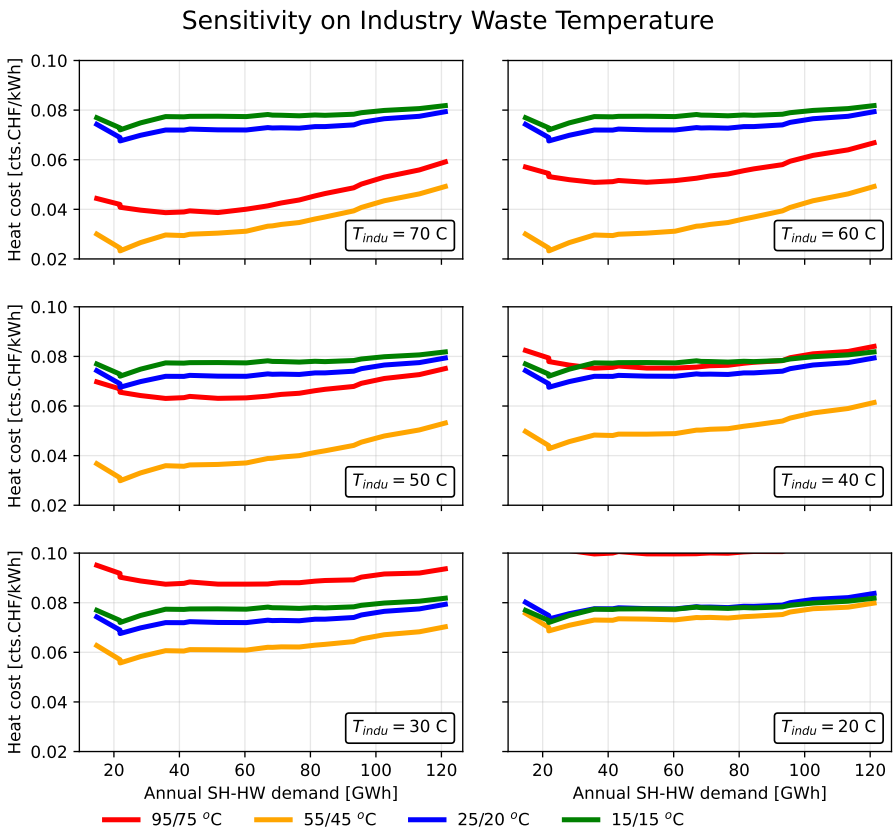

Figure 3.14: Final cost of the heat delivered by the DHN in function of the size of the network and for different temperatures of industry waste.

2.3.1), the program will generate a design of the network. The output is also a *GeoPachage* file.

In order to improve the user experience, the functions are implemented on a web interface using the open-source app framework *Streamlit*. The app can be accessed using this link : https://ipese-web.epfl.ch/pypipes. The GitHub project can be found here.

Chapter 4

Discussion

The previous chapter compared four configurations of DHN in order to integrate the heat waste of *Novelis* to Sierre's heating system.

It has been first shown that the DHN working at a temperature of 95/75 °C is the less attractive solution. Whether it is in terms of final heat cost or emissions, the low COP and the high cost of operation do not make this configuration competitive. This temperature level could be nevertheless favourable to a heat waste temperature higher than what is considered in this study. However, when dealing with high temperature heat waste (e.g > 100 °C), the use of Organic Ranking Cycle could be considered.

Then, the heat cost highly depends on the temperature released by the industry. We have also considered that this heat was provided for free, since the connection between Sierre and *Novelis* is a win-win agreement. However, the contract between both entities can be different. On the one side, *Novelis* could sell the heat to the city, but it can also be envisioned that *Novelis* would pay the city to evacuate the heat.

Despite the fact that the cost of the 15/15 °C network is 31% higher than the best configuration (with T_{indu} at 30 °C), this technology is able to supply cold via the same system. For now, the air conditioning in housing remains relatively rare, but that will surely evolve. According to [27], the cooling demand for households is three times higher in 2021 (100 cooling degree days) than in 1979 (37 cooling degree days). With conventional DHN, an additional pipe network is required to supply cooling whereas the 15 °C CO_2 network has the advantage of being used in summer as free cooling, meaning that no extra infrastructure is required. In fact, at the central plant, water from a river or lake can be used to extract the heat of the CO_2 through an exchanger without any refrigeration system.

One of the main consequence of using low temperature network, is the needs of a decentralized utility. It should be noted that a heat pump requires, in general, more space than natural gas or heating oil boiler. Therefore, the space available in some buildings may not be sufficient. It could be the case for the city center where the density of buildings is higher. A solution that could be imagined

is to install a substation that increases the temperature for the entire district.
Concerning the reduction of emissions following the replacement of fossil fuel utilities, the actual electric mix is considered. With the district analysed in this study, the electricity consumed by the heat pumps is 1.5 to 2 times greater than the district's annual electric consumption. The integration of PV panels could increase the self-sufficiency of the city.

4.1 Future perspectives

In order to have more precise results, some aspects of the methodology could be adapted or added. Firstly, the integration of the cooling demand would allow us to bring to the fore the advantage of using CO_2 to supply the cold. Then, concerning the optimization of the piping path, it is possible to also use the routing algorithm inside the districts instead of the length estimation formula. Alternatively, after the selection of the best districts, the routing algorithm could be used on smaller subdistrict. It would result in a more detailed network. Moreover, the possibility of connecting more than one industry of heat source to the same network would be an advantage for the integration of multiple renewable sources.

Chapter 5

Conclusion

All along this study, we have developed a methodology to design a District Heating Network in a city territory. It started from the evaluation of the energy demand of the buildings (Section 2.1), followed by the creation of districts with an internal network (Section 2.2) and ended with the connection of all districts to the industry (Section 2.3). This methodology is applied to the city of Sierre in order to recycle the the heat waste from *Novelis*.

In Section 2.1, *Qbuildings*, the tool developed in IPESE laboratory, yields that Sierre's energy demand amounts to 177 GWh/year for Space Heating and 32 GWh/year for Hot Water production. The comparisons with the Territorial Energy Master Plan commissioned by the city has enabled us to verify and correct some of the assumptions. The results of *Qbuildings* deviated from the TEMP by 35% for the Hot Water and by -10% for the Space Heating demand. Nevertheless, the TEMP is also based on a statistical approach, meaning that it remains difficult to estimate how close to the reality these results are. This analysis allows us, however, to point out that *Qbuildings*'s method, only based on open data, leads to results close to those yielded by a detailed study like the TEMP.

Once the demand is computed, the length of the network inside each district was estimated using a formula calibrated with the gas grid. The estimation can reach a relative error smaller than 5% for the main districts of the city. The cost of the network in the district makes possible to assign a grade to each of them and select the areas that will be connected to the industry. The routing algorithm, that uses the function of *Open Street Map*, is a simple and efficient way to draw realistic network's path. On top of that, the method enables us to manually add constraints about the roads that the network can or cannot use.
The building's heat demand profile computed by *Qbuildings* helps to compute the investment and operating cost of central and decentralized heat pumps. The four temperature levels selected for the case study result in different levels of decentralization. The share of the power that is supplied by the decentralized unit is 25% for the 15/15 °C network, 21% for 25/20 °C and 5% for the 55/45 °C scenario. The latter has the best global COP, which contributes to minimize the operating costs of the system. The global COP is directly correlated to the emissions of the system. It has been

shown that the connection to the DHN permits to reduce the Global Warming Potential linked to the heating system by 88% to 96%. At the scale of the city, when 50% of Sierre is supplied by the DHN, the total emissions of the city are reduced by 55%. The emission avoidance depends slightly on the type of DHN. However, the electric consumption of Sierre is double when 50% of the buildings are connected to the 95/75 °C network, while it increases by 72% with the CO_2 network. A large integration of PV panels on the city's roofs would lead Sierre towards self-sufficiency.
The 55/45 °C network is the configuration that achieves the lowest final heat price. Since the operating cost accounts, in any case, for more than 50% of the heat price, a good COP leads to a reduction of the final bill. It is the case of the 55/45 °C network. However, the cost relies greatly on the industry temperature waste. The sensitivity analysis on the industry temperature shows that when it is approaching the 20 °C, the anergy and CO_2 network become as attractive as the 55/45 °C network. Moreover, these low temperature networks have the advantage of being able to supply cold with the same infrastructure. Finally, many low temperature heat sources all over the city could also be integrated to the system, such as a commercial center or ice hockey ring. We can imagine that the smart synergy between the consumer, the heat sources, PV panels and energy storage could lead towards an energy autonomy.

Bibliography

[1] Henrik Lund, Poul Alberg Østergaard, Tore Bach Nielsen, Sven Werner, Jan Eric Thorsen, Oddgeir Gudmundsson, Ahmad Arabkoohsar, and Brian Vad Mathiesen. Perspectives on fourth and fifth generation district heating. *Energy*, 227:120520, 2021.

[2] Luc Girardin. A GIS-based methodology for the evaluation of integrated energy systems in urban area. page 218, 2012.

[3] Samuel Henchoz. Potential of refrigerant based district heating and cooling networks. page 249, 2016.

[4] Nico Rohrbach, Martin Hertach, Daniel Binggeli, Andreas Hurni, and Anton Sres. Bases et explications sur les réseaux thermiques Informations sur le document. Technical report, Hochschule Luzern.

[5] Office fédéral de la statistique. Domaine énergétique. https://www.bfs.admin.ch/.

[6] Office fédéral de la statistique. Locataires / propriétaires. https://www.bfs.admin.ch/.

[7] Novelis. https://www.novelis.com/.

[8] dominiqueheller. Net Zero Lab Valais – Novelis Sierre to develop Carbon-Neutral Solutions for Aluminium Manufacturing. https://www.novelis.com/net-zero-lab-valais/, February 2022.

[9] Cité de l'énergie GOLD. https://www.sierre.ch/fr/cite-energie-gold-2144.html.

[10] B. Dong, S. Bang Lee, and M. Haji Sapar. A holistic utility bill analysis method for baselining whole commercial building energy consumption in singapore. *Energy and Buildings*, 37(2):167–174, 2005. Cited By :47.

[11] Raluca-Ancuta Suciu. Fifth generation district energy systems for low carbon cities. page 218, 2019.

[12] Henrik Lund, Sven Werner, Robin Wiltshire, Svend Svendsen, Jan Eric Thorsen, Frede Hvelplund, and Brian Vad Mathiesen. 4th Generation District Heating (4GDH): Integrating smart thermal grids into future sustainable energy systems. *Energy*, 68:1–11, 2014.

[13] Céline Weber and Daniel Favrat. Conventional and advanced CO2 based district energy systems. *Energy*, 35(12):5070–5081, 2010.

[14] Samuel Henchoz, Daniel Favrat, and Céline Weber. Performance and profitability perspectives of a CO2 based district energy network in geneva's city center. 2012.

[15] Raluca Suciu, Luc Girardin, and François Maréchal. Energy integration of CO2 networks and power to gas for emerging energy autonomous cities in Europe. *Energy*, 157:830–842, August 2018.

[16] Jérémy Unternährer, Stefano Moret, Stéphane Joost, and François Maréchal. Spatial clustering for district heating integration in urban energy systems: Application to geothermal energy. *Applied Energy*, (15 March 2017):15. 749–763, 2017.

[17] Federal Statistical Office (FSO). https://www.bfs.admin.ch/.

[18] Stefan Schneider, Jad Khoury, Bernard M. Lachal, and Pierre Hollmuller. Geo-dependent heat demand model of the swiss building stock: method, results and example of application. Technical report, SCCER Future Energy Efficient Buildings Districts, 2018. ID: unige:103112.

[19] The history of district heating. www.history.vattenfall.com/.

[20] History of District Heating, March 2017.

[21] Katinka Johansen and Sven Werner. Something is sustainable in the state of Denmark: A review of the Danish district heating sector. *Renewable and Sustainable Energy Reviews*, 158:112117, 2022.

[22] QM Fernwärme, editor. *Guide de planification Chauffage à distance*. EnergieSchweiz, Bundesamt für Energie BFE, Ittigen, version 1.2 edition, 26.

[23] Vladislav Masatin, Eduard Latõšev, and Anna Volkova. Evaluation factor for district heating network heat loss with respect to network geometry. *Energy Procedia*, 95:279–285, 2016.

[24] Francesca Belfiore. District heating and cooling systems to integrate renewable energy in urban areas. page 250, 2021.

[25] Conférence de coordination des services de la construction et des immeubles des maîtres d'ouvrage publics KBOB. Données écobilans dans la construction. https://www.kbob.admin.ch/.

[26] Marquage de l'électricité. https://www.strom.ch/fr/services/marquage-de-lelectricite.

[27] Heating of buildings decreasing, cooling increasing. https://ec.europa.eu/eurostat/web/products-eurostat-news/-/ddn-20220531-1.